

UNCLASSIFIED

AD 406 092

DEFENSE DOCUMENTATION CENTER

FOR

SCIENTIFIC AND TECHNICAL INFORMATION

CAMERON STATION, ALEXANDRIA, VIRGINIA



UNCLASSIFIED

NOTICE: When government or other drawings, specifications or other data are used for any purpose other than in connection with a definitely related government procurement operation, the U. S. Government thereby incurs no responsibility, nor any obligation whatsoever; and the fact that the Government may have formulated, furnished, or in any way supplied the said drawings, specifications, or other data is not to be regarded by implication or otherwise as in any manner licensing the holder or any other person or corporation, or conveying any rights or permission to manufacture, use or sell any patented invention that may in any way be related thereto.

Contract NObsr-89265

Project Serial Number SF001-03-01, Task 8100

TECHNICAL MEMORANDUM

AN ANALYTIC SOLUTION TO THE SOUND PRESSURE FIELD
RESULTING FROM A PLANE WAVE INCIDENT ON A CYLINDER
AND CONCENTRIC CYLINDRICAL SECTION -
COMPUTATIONAL TECHNIQUES

Prepared for

The Bureau of Ships
Code 689B

This technical memorandum contains partial results
obtained during an analytical study of the sound
field near a dome-baffle-transducer complex.

8 May 1963

Prepared by:

G. S. Mills

G. S. Mills

W. C. Moyer

W. C. Moyer

Alice M. Spitzer

Alice M. Spitzer

I. INTRODUCTION

This memorandum describes the computational techniques used in the numerical evaluation of a solution to the sound pressure field resulting from a plane wave incident on a cylinder and concentric cylindrical section. The analytical development of the solution is given in a separate technical memorandum (1).

In the numerical evaluation of the solution to the baffle-transducer sound field, values of Bessel and Neumann functions are required for a large range of order and argument. Consequently, an initial requirement for the numerical evaluation of the solution was to obtain the required values of the Bessel and Neumann functions. Published values of the functions are only available for a limited range of order and argument. Furthermore, the use of the asymptotic expressions available for evaluating the functions is limited to small ranges of order and argument unless a large number of significant figures is available. Techniques suitable for evaluating Bessel and Neumann functions on a small digital computer have therefore been developed. These techniques, which are described in (2) and (3), are a part of the computational procedure described in this memorandum.

For the purpose of numerical evaluation it is convenient to divide the baffle-transducer sound field solution into several quantities which may be computed individually. The computations of these quantities then become sub-routines of a master program for evaluating the solution. The separation of the solution into these quantities is described in Section II of this memorandum.

The coefficients which appear in the solution for the baffle-transducer sound field arise in the form of an infinite set of inhomogeneous equations. For the numerical evaluation of the solution it is necessary to approximate the infinite set of coefficients

by a truncated set of coefficients. This procedure is discussed in Section III. The validity of the approximation is supported by demonstrating the convergence of the individual coefficients of a finite set to stable values independent of the size of the set of coefficients evaluated once the set is large enough.

In the last section some numerical results for the solution are presented. Since experimental measurements of the response of scanning sonar equipments to an incident noise field are given in terms of self-noise directivity patterns, the sound field at the transducer computed from the baffle-transducer sound field solution is presented in this form.

Appendix A contains a description of the technique used in evaluating a finite set of simultaneous equations. The solution of such a set of equations occurs in the numerical evaluation of the solution of the baffle-transducer sound field.

Appendix B contains a description of the computer program used for the numerical evaluation of the baffle-transducer sound field.

In Appendix C a description is given of the technique employed in simulating the beam-forming process on a digital computer.

II. A COMPUTATIONAL FORM FOR THE SOLUTION

In this section the form of the analytical solution to the baffle-transducer sound field given in (1) will be expressed in a form suitable for computational purposes. The data to be obtained in a numerical evaluation of the solution includes the pressure amplitude and phase of the sound field at various points in the vicinity of the baffle-transducer.

The form of the solution given in (1) is

$$p_1 = \sum_{n=0}^{\infty} E_n \left[J_n(kr) - \frac{J'_n(ka)}{N'_n(ka)} N_n(kr) \right] \cos n\theta e^{-i\omega t} \quad (1)$$

where p_1 is the sound pressure in the annular region between the baffle and transducer (see Figure 1), $J_n(kr)$ and $N_n(kr)$ are the Bessel and Neumann functions of order n respectively, the primes indicate differentiation with respect to the argument, k is the wave number of the incident wave ($k = 2\pi/\lambda$, where λ is the wavelength), and E_n is determined from the relation

$$E_n \left[J_n(kb) - \frac{J'_n(ka)}{N'_n(ka)} N_n(kb) \right] =$$

$$\frac{\epsilon_n}{2\pi} \varphi \sum_{\ell=0}^{\infty} \left[E_{\ell} \left\{ J'_{\ell}(kb) - \frac{J'_{\ell}(ka)}{N'_{\ell}(ka)} N'_{\ell}(kb) \right\} \sum_{j=0}^{\infty} \left\{ \frac{j}{\ell} \right\} \frac{J_j(kb) + iN_j(kb)}{J'_j(kb) + iN'_j(kb)} \frac{\epsilon_j}{2\pi} \varphi \left\{ \frac{n}{j} \right\} \right]$$

$$+ \frac{\epsilon_n}{2\pi} \varphi \sum_{j=0}^{\infty} \left\{ \epsilon_j i^j J_j(kb) - \epsilon_j i^j J'_j(kb) \frac{J_j(kb) + iN_j(kb)}{J'_j(kb) + iN'_j(kb)} \right\} \left\{ \frac{n}{j} \right\} \cdot \quad (2)$$

This equation is an infinite set of inhomogeneous equations of the form

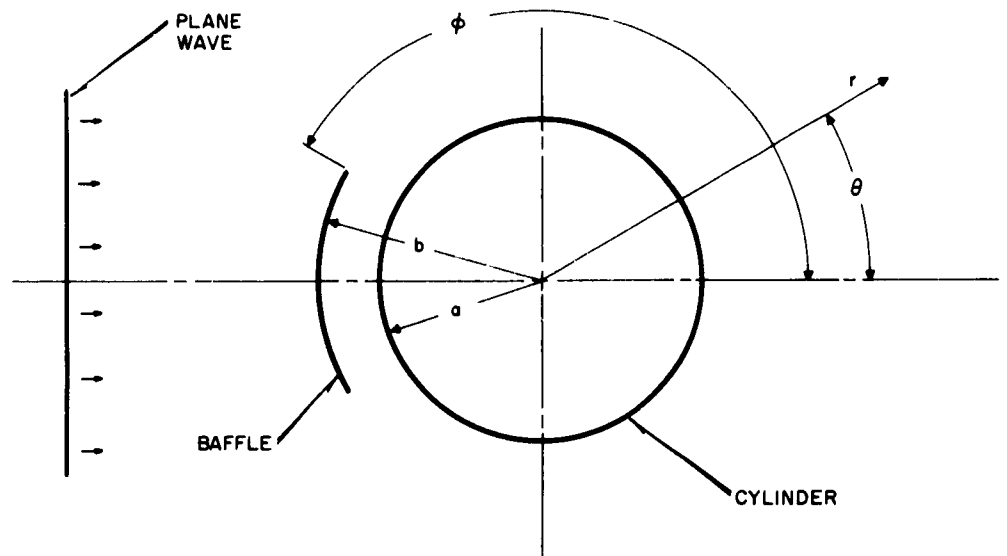


**Fig. 1 - GEOMETRY OF THE INFINITE-LENGTH
CYLINDER AND CYLINDRICAL SHELL**

$$E_n = \sum_{l=0}^{\infty} \alpha_{ln} E_l = \beta_n, \quad \text{where} \quad (3)$$

α_{ln} and β_n are constants.

The expression for the pressure given in eq. (1) is a complex quantity, hence the magnitude of the pressure can be written as

$$|p_1| = \left[\left[\sum_n R_n \cos n\theta \right]^2 + \left[\sum_n I_n \cos n\theta \right]^2 \right]^{\frac{1}{2}}, \quad (4)$$

where R_n represents the real part of eq. (1) and I_n is the imaginary part of eq. (1). The phase ϕ of the pressure field at any point can be written as

$$\phi = \tan^{-1} \frac{\sum_n I_n \cos n\theta}{\sum_n R_n \cos n\theta}. \quad (5)$$

$|p_1|$ and ϕ are the quantities that are to be evaluated.

The real and imaginary parts of p_1 (R and I) are determined from the expression for E_n given by eq. (2). R and I can be written as

$$R_n = K_n (\beta_n D_n^R - \alpha_n D_n^I) \quad (6)$$

and

$$I_n = K_n (\beta_n D_n^I + \alpha_n D_n^R), \quad (7)$$

where

$$K_n = \frac{\beta_n J_n(kr) - \alpha_n N_n(kr)}{\alpha_n^2 + \beta_n^2} \quad , \quad (8)$$

$$\alpha_n = J'_n(ka) = 1/2 [J_{n-1}(ka) - J_{n+1}(ka)] \quad , \quad \text{and} \quad (9)$$

$$\beta_n = N'_n(ka) = 1/2 [N_{n-1}(ka) - N_{n+1}(ka)] \quad . \quad (10)$$

D_n^R and D_n^I are determined from the following sets of simultaneous equations.

$$\sum_l D_l^R (A_l X_l^n - \delta_n^l B_n \beta_n) - \sum_l D_l^I (A_l Y_l^n - \delta_n^l B_n \alpha_n) = F_n \quad (11)$$

$$\sum_l D_l^R (A_l Y_l^n - \delta_n^l B_n \alpha_n) + \sum_l D_l^I (A_l X_l^n - \delta_n^l B_n \beta_n) = G_n \quad (12)$$

$$F_n = - \frac{\pi}{\varphi} \left[\sum_{l=0,2,4,\dots} \epsilon_l (-1)^{\frac{l}{2}} L_l b_l \left\{ \begin{matrix} n \\ l \end{matrix} \right\} \right. \\ \left. + \sum_{l=1,3,5,\dots} \epsilon_l (-1)^{\frac{l+1}{2}} L_l a_l \left\{ \begin{matrix} n \\ l \end{matrix} \right\} \right] \quad (13)$$

$$G_n = -\frac{\pi}{\varphi} \left[\sum_{l=0,2,4,\dots} \epsilon_l (-1)^{\frac{l}{2}} L_l a_l \left\{ \begin{matrix} n \\ l \end{matrix} \right\} + \sum_{l=1,3,5,\dots} \epsilon_l (-1)^{\frac{l-1}{2}} L_l b_l \left\{ \begin{matrix} n \\ l \end{matrix} \right\} \right] \quad (14)$$

$$X_l^n = \sum_j \epsilon_j \left\{ \begin{matrix} n \\ j \end{matrix} \right\} \left\{ \begin{matrix} j \\ l \end{matrix} \right\} (\beta_l M_j + \alpha_l L_j) \quad (15)$$

$$Y_l^n = \sum_j \epsilon_j \left\{ \begin{matrix} n \\ j \end{matrix} \right\} \left\{ \begin{matrix} j \\ l \end{matrix} \right\} (\alpha_l M_j - \beta_l L_j) \quad (16)$$

$$A_l = \frac{(a_l \beta_l - \alpha_l b_l)}{\alpha_l^2 + \beta_l^2} \quad (17)$$

$$B_l = \frac{4\pi^2 [J_l(kb)\beta_l - \alpha_l N_l(kb)]}{\epsilon_l \varphi^2 (\alpha_l^2 + \beta_l^2)} \quad (18)$$

$$L_j = \frac{b_j J_j(kb) - a_j N_j(kb)}{a_j^2 + b_j^2} \quad (19)$$

$$M_j = \frac{a_j J_j(kb) + b_j N_j(kb)}{a_j^2 + b_j^2} \quad (20)$$

$$a_n = J'_n(kb) = 1/2 [J_{n-1}(kb) - J_{n+1}(kb)], \quad a_0 = -J_1(kb) \quad (21)$$

$$b_n = N'_n(kb) = 1/2 [N_{n-1}(kb) - N_{n+1}(kb)], \quad b_0 = -N_1(kb) \quad (22)$$

$$\left\{ \begin{matrix} n \\ j \end{matrix} \right\} = \frac{\sin|n-j|\varphi}{|n-j|\varphi} + \frac{\sin(n+j)\varphi}{(n+j)\varphi} \quad (23)$$

$$\delta_n^l = 1, \quad l = n \quad \text{and} \quad \delta_n^l = 0, \quad l \neq n \quad (24)$$

The computation of each of these quantities is accomplished in sub-routines of a master program for evaluating the solution given in eq. (1). The master program and sub-routines are described in Appendix B.

III. COMPUTATIONAL TECHNIQUES

The primary difficulty in the numerical evaluation of the baffle-transducer sound field solution, eq. (1), is the determination of the coefficients, E_n , given in eq. (3). The analytical representation of E_n is an infinite set of inhomogeneous equations in which each coefficient is given in terms of itself and the other coefficients. A qualitative examination of the functional forms of the quantities $\alpha_{\ell n}$ and β_n (see equations (2) and (3)) shows that the factors $\left\{ \begin{matrix} j \\ \ell \end{matrix} \right\}$ and $\left\{ \begin{matrix} n \\ j \end{matrix} \right\}$ will have a tendency to cause the major contribution to the sum on ℓ to arise for values of ℓ in the vicinity of n . (These quantities have convergence characteristics similar to the function $\frac{\sin x}{x}$.) One would expect, therefore, that it should be possible to obtain accurate numerical values for the first N of the coefficients E_n if the indices in the summation (n and ℓ) in eq. (3) are restricted to a finite number $M \geq N$. Equation (3) then becomes a set of M inhomogeneous equations in M unknowns which can be evaluated numerically (see Appendix A). Equation (1) can then be evaluated. The number, N , of accurate coefficients required is determined by the convergence of eq. (1). The number, M , of coefficients which must be included in eq. (3) to obtain accurate values for the first N of the E 's is determined by the convergence effects of the factors $\left\{ \begin{matrix} j \\ \ell \end{matrix} \right\}$ and $\left\{ \begin{matrix} n \\ j \end{matrix} \right\}$.

This technique has been substantiated by determining values of the coefficients for various values of M , assuming a fixed value for N . In this case values of D_n^R and D_n^I , the real and imaginary parts of E_n , were computed for $N = 50$ and $M = 100$ and $M = 150$. The results of this comparison are given in Table 1. It is seen that the coefficients D_n^I and D_n^R have reached reasonably stable values

for $M = 100$, i.e., for $M = 100$ and $M = 150$ the values of the coefficients are practically the same. The pressure, eq. (1), was then evaluated using each of the sets of coefficients. A comparison of the values obtained is given in Table 2. It can be seen that, for at least the particular set of parameters used in this evaluation (k, a, b, φ), the results are nearly identical. Hence, the smaller set of simultaneous equations ($M = 100$) is satisfactory for the evaluation of eq. (1). The pressure amplitude for this case is shown in Figure 2.

The solution was verified by comparing numerical results for the case of $\varphi = 180^\circ$, i.e., zero baffle width, with the results of an evaluation of the classical solution to the sound field resulting from a plane wave incident on an infinite length rigid cylinder. The pressure amplitudes and phases obtained from the two solutions are compared in Table 3. In addition, the pressure amplitude for the case of zero baffle width is shown in Figure 3. It can be seen that both pressure amplitude and phase compare quite favorably for the two solutions. The agreement of the baffle-transducer sound field solution with the simple cylinder solution represents a substantial verification of the techniques used in the baffle-transducer sound field computation.

TABLE I

A COMPARISON OF THE COEFFICIENTS D_n^R AND D_n^I COMPUTED FROM
TWO DIFFERENT SETS OF M SIMULTANEOUS EQUATIONS

$$\begin{aligned} \varphi &= 165^\circ \\ ka &= 23.56 \quad b = 90'' \end{aligned}$$

	M=100	M=150
	D_n^R and D_n^I	D_n^R and D_n^I
D_0^R	.0350984	.0422946
D_0^I	.505417	.492501
D_1^R	-.946866	-.920642
D_1^I	.0566811	.074510
D_2^R	-.0635814	-.080683
D_2^I	-.898818	-.874366
D_3^R	.810396	.788585
D_3^I	-.0689177	-.0846728
D_4^R	.0998481	.113703
D_4^I	.719360	.700551
D_5^R	-.615209	-.599812
D_5^I	.142809	.154100
D_6^R	-.202259	-.209673

TABLE I (Cont'd)

	M=100	M=150
	D_n^R and D_n^I	D_n^R and D_n^I
D_6^I	-.508902	-.496312
D_7^R	.403891	.393362
D_7^I	-.271244	-.275685
D_8^R	.355985	.356973
D_8^I	.302783	.293452
D_9^R	-.223956	-.214539
D_9^I	.448126	.446056
D_{10}^R	-.533861	-.529582
D_{11}^I	-.168091	-.157640
D_{11}^R	.178131	.165982
D_{11}^I	-.580330	-.575617
D_{12}^R	.657598	.655479
D_{12}^I	.147571	.137767
D_{13}^R	-.159424	-.144676
D_{13}^I	.642323	.640644

TABLE I (Cont'd)

	M=100	M=150
	D_n^R and D_n^I	D_n^R and D_n^I
D_{14}^R	-.705866	-.707561
D_{14}^I	-.140504	-.126188
D_{15}^R	.114500	.102767
D_{15}^I	-.685095	-.689819
D_{16}^R	.662697	.667817
D_{16}^I	.0750578	.0671874
D_{17}^R	.00130028	.00585412
D_{17}^I	.645939	.650207
D_{18}^R	-.419410	-.418552
D_{18}^I	.972592	.973815
D_{19}^R	-.174535	-.177493
D_{19}^I	-.726803	-.725742
D_{20}^R	.820809	.817848
D_{20}^I	-.227778	-.233440
D_{21}^R	.239705	.249350

TABLE I (Cont'd)

	M=100	M=150
	D_n^R and D_n^I	D_n^R and D_n^I
D_{21}^I	.927288	.925269
D_{22}^R	-1.01166	-1.01429
D_{22}^I	.202999	.216407
D_{23}^R	-.135361	-.148348
D_{23}^I	-1.04896	-1.05851
D_{24}^R	1.13030	1.14290
D_{24}^I	.283495	.282009
D_{25}^R	.0245484	.023998
D_{25}^I	1.02915	1.04665
D_{26}^R	-.957032	-.975116
D_{26}^I	.477974	.474935
D_{27}^R	-.105330	-.0932969
D_{27}^I	-.969128	-.974884
D_{28}^R	1.02553	1.02458
D_{28}^I	-.161015	-.150995

TABLE I (Cont'd)

	M=100	M=150
	D_n^R and D_n^I	D_n^R and D_n^I
D_{29}^R	.164267	.159353
D_{29}^I	1.13682	1.13368
D_{30}^R	-1.10410	-1.10283
D_{30}^I	-.381412	-.377503
D_{31}^R	.0958926	.100168
D_{31}^I	-1.28357	-1.28582
D_{32}^R	1.18401	1.18433
D_{32}^I	.276265	.286122
D_{33}^R	-.355106	-.367154
D_{33}^I	.962977	.954309
D_{34}^R	-.721675	-.703262
D_{34}^I	-.255979	-.260411
D_{35}^R	-.0542341	-.0653916
D_{35}^I	-.598181	-.578178
D_{36}^R	.291690	.222372
D_{36}^I	-2.40690	-2.42268

TABLE I (Cont'd)

	M=100	M=150
	D_n^R and D_n^I	D_n^R and D_n^I
D_{37}^R	.386058	.409269
D_{37}^I	1.09323	1.10617
D_{38}^R	-1.28874	-1.31347
D_{38}^I	.214077	.221761
D_{39}^R	.0858212	.0968643
D_{39}^I	-1.33621	-1.35774
D_{40}^R	1.09312	1.10185
D_{40}^I	.306737	.326212
D_{41}^R	-.217383	-.238223
D_{41}^I	.809808	.805783
D_{42}^R	-.686704	-.690052
D_{42}^I	1.03805	1.03123
D_{43}^R	-.202972	-.204207
D_{43}^I	-.947747	-.915456
D_{44}^R	1.13444	1.10941

TABLE I (Cont'd)

	M=100	M=150
	D_n^R and D_n^I	D_n^R and D_n^I
D_{44}^I	-.102192	-.137711
D_{45}^R	-.0708431	-.0181885
D_{45}^I	1.12419	1.14803
D_{46}^R	-.983872	-1.05459
D_{46}^I	-.101903	-.101561
D_{47}^R	.0974928	.189896
D_{47}^I	-.831941	-.868575
D_{48}^R	1.84956	1.77326
D_{48}^I	.767130	.822620
D_{49}^R	.133107	.245294
D_{49}^I	1.11337	.989887

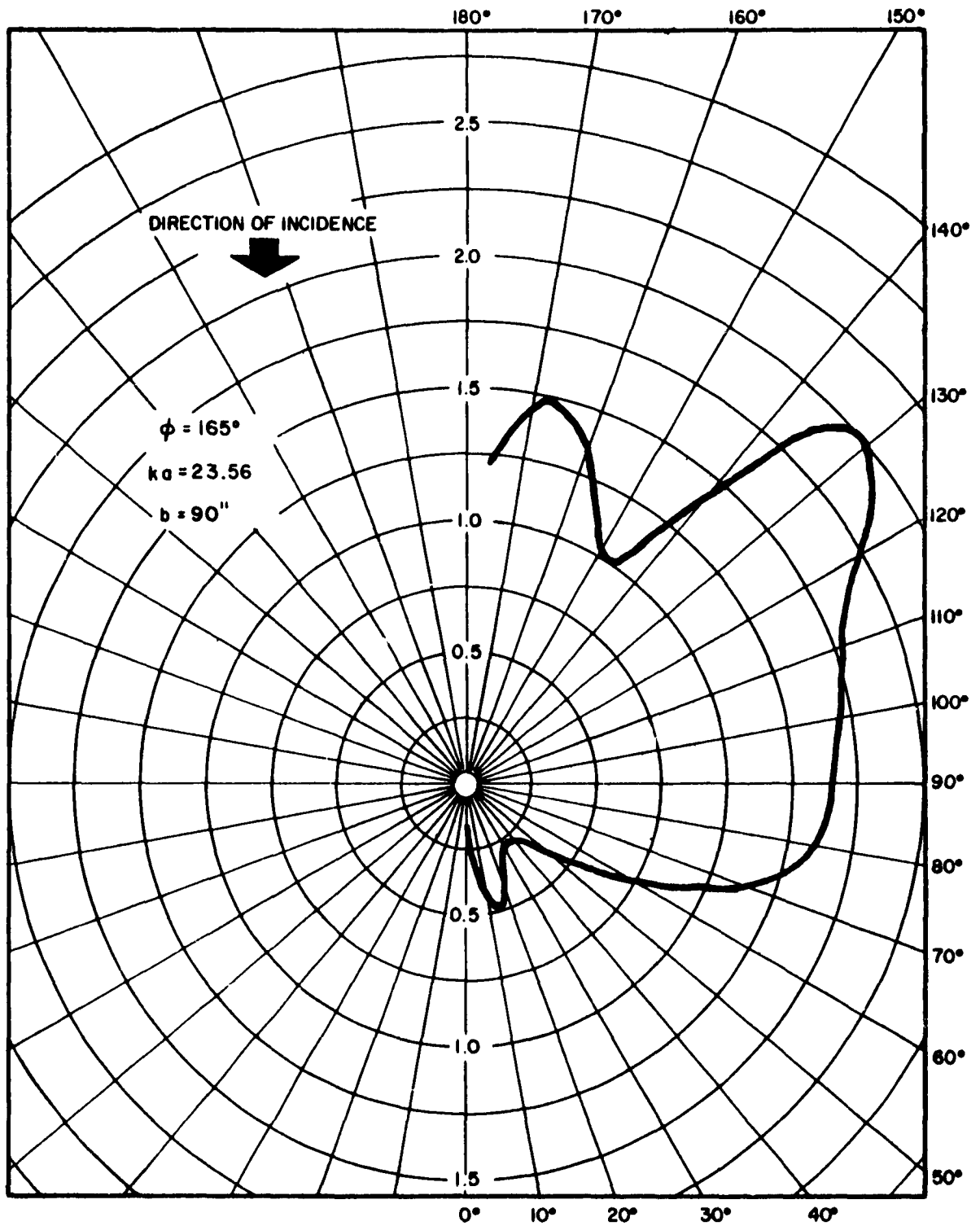


Fig. 2 - PRESSURE AMPLITUDE OF BAFFLE-TRANSDUCER SOUND FIELD AT THE TRANSDUCER FACE

REFERRED TO UNIT AMPLITUDE INCIDENT WAVE

TRACOR, INC DWG. A2000-175
 AUSTIN, TEXAS 8/18/68 WGM/cwc

TABLE II

A COMPARISON OF PRESSURE AMPLITUDE AND PHASE COMPUTED
FROM TWO DIFFERENT SETS OF SIMULTANEOUS EQUATIONS

$$\varphi = 165^\circ$$

$$ka = 23.56$$

$$b = 90''$$

θ	M=100		M=150	
	Amplitude	Phase	Pressure	Phase
3.75°	.18266	315.073°	.18429	315.131°
11.25°	.45290	140.602°	.45404	140.575°
18.75°	.47306	318.353°	.47510	318.038°
26.25°	.36042	130.972°	.36218	130.687°
33.75°	.25358	272.848°	.25616	273.545°
41.25°	.27240	61.582°	.27226	62.437°
48.75°	.35334	248.045°	.35656	248.656°
56.25°	.54702	95.670°	.55156	95.746°
63.75°	.89906	287.212°	.90664	287.242°
71.25°	1.19226	108.452°	1.19968	108.373°
78.75°	1.34960	282.039°	1.36010	281.874°
86.25°	1.38304	91.808°	1.39450	91.663°
93.75°	1.41814	259.444°	1.43102	259.486°
101.25°	1.47368	75.081°	1.48828	75.082°
108.75°	1.53762	265.191°	1.55680	264.967°
116.25°	1.63716	111.243°	1.65322	110.663°
123.75°	1.86178	322.297°	1.87308	321.559°
131.25°	2.00686	177.030°	2.00810	176.244°
138.75°	1.52218	44.850°	1.51294	43.945°
146.25°	1.01020	320.219°	1.00212	319.754°
153.75°	1.10244	257.328°	1.09818	256.083°
161.25°	1.39846	225.442°	1.36004	224.134°
168.75°	1.47772	178.390°	1.44370	177.096°
176.25°	1.22224	210.162°	1.19062	208.776°

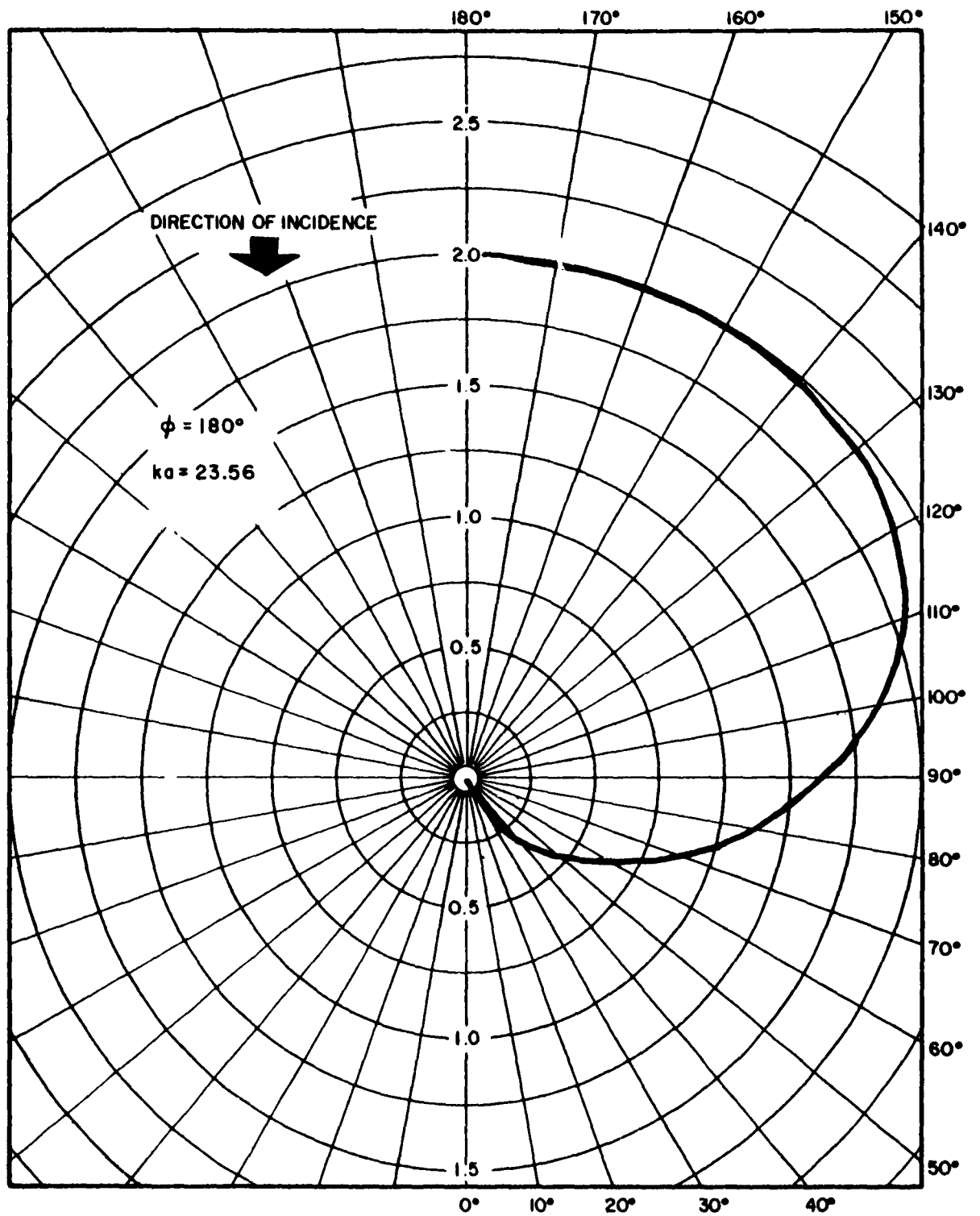


Fig. 3 - PRESSURE AMPLITUDE OF BAFFLE-TRANSDUCER SOUND FIELD AT THE TRANSDUCER FACE FOR THE CASE OF ZERO BAFFLE

REFERRED TO UNIT AMPLITUDE INCIDENT WAVE

TRACOR, INC. DWG. A 2000-176
 AUSTIN, TEXAS 6/18/63 WCM/GWC

TABLE III

COMPARISON OF PRESSURE AMPLITUDE AND PHASE FOR THE CASE OF
ZERO BAFFLE WIDTH OBTAINED FROM THE BAFFLE-TRANSDUCER
SOLUTION AND THE CLASSICAL SOLUTION FOR A PLANE
WAVE INCIDENT ON A RIGID CYLINDER

Angle θ	Classical Solution		Transducer-Baffle Solution	
	Amplitude	Phase	Pressure	Phase
3.75°	.0217562	312.606°	.0217520	312.594
11.25°	.0665575	131.703°	.0665674	131.702
18.75°	.115481	309.974°	.115477	309.970
26.25°	.171593	127.432°	.171602	127.426
33.75°	.238627	304.140°	.238633	304.137
41.25°	.320976	120.149°	.320974	120.144
48.75°	.423516	295.508°	.423511	295.506
56.25°	.550975	110.301°	.550969	110.297
63.75°	.706252	284.682°	.706250	284.677
71.25°	.888185	98.990°	.888185	98.983
78.75°	1.08940	273.814°	1.08940	273.807
86.25°	1.29609	90.058°	1.29611	90.049
93.75°	1.49085	268.957°	1.49085	268.946
101.25°	1.65788	92.060°	1.65790	92.048
108.75°	1.78789	281.201°	1.78788	281.190
116.25°	1.87926	118.4623°	1.87925	118.451
123.75°	1.93577	326.111°	1.93574	326.100
131.25°	1.96302	186.570°	1.96303	186.557
138.75°	1.97014	62.340°	1.97016	62.328
146.25°	1.97546	315.659°	1.97549	315.648
153.75°	1.99297	227.878°	1.99297	227.868
161.25°	1.99995	160.175°	1.99996	160.167
168.75°	1.99268	114.654°	1.99270	114.649
176.25°	1.99787	91.707°	1.99790	91.703

IV. NUMERICAL RESULTS

The numerical evaluation of the analytical solution to the baffle-transducer complex has been completed for several values of the parameters. The solution is presently being studied as a function of incident wave frequency and angular extent of the baffle. The parametric analysis of the solution will also include the effects of relative baffle-transducer spacing, baffle impedance, and transducer diameter. The range of parameters to be studied is:

1. Incident wave frequency, 1 kc \rightarrow 15 kc
2. Angular extent of the baffle, $0^\circ \rightarrow 120^\circ$
3. Baffle-transducer spacing, 1 ft. \rightarrow 20 ft.
4. Baffle surface impedance, the limiting cases of perfectly rigid and perfectly absorbing surfaces will be analyzed. If experimentally measured values of surface impedance are available, these can also be included in the parametric analysis.
5. Transducer diameter, 2.7 ft. \rightarrow 16 ft.

The response of a sonar to the anisotropic sound field resulting from the diffraction of a plane wave by the baffle-transducer is obtained by (a) computing the pressure amplitude and phase of the diffracted sound field from eq. (1) at points on the transducer face corresponding to transducer elements, and (b) using this pressure amplitude and phase information as individual transducer element responses in a simulated sonar beam forming process (see Appendix C). The beam forming process has been made an optional sub-routine in the master program for evaluating eq. (1). The numerical results of an evaluation of p_1 , eq. (1) are then obtainable

either in the form of beam responses of a scanning sonar equipment or as pressure magnitudes and phases at points on the transducer corresponding to element faces. A parametric analysis of the effect of the baffle-transducer diffracted sound field on sonar beam forming processes is then easily obtained.

Some numerical results for the total diffracted sound field of the baffle-transducer for various parameter values are shown in Figures 4 - 23. Both the pressure amplitude and beam pattern are shown for each set of parameter values studied. For these results, the transducer diameter, relative spacing of the transducer and baffle, and baffle surface impedance are each constant. The angular extent of the baffle has been varied from 0° to 120° (φ varied from 180° to 120°) for values of $ka = 8.77$ (Figures 4 - 13) and 17.54 (Figures 14 - 23).

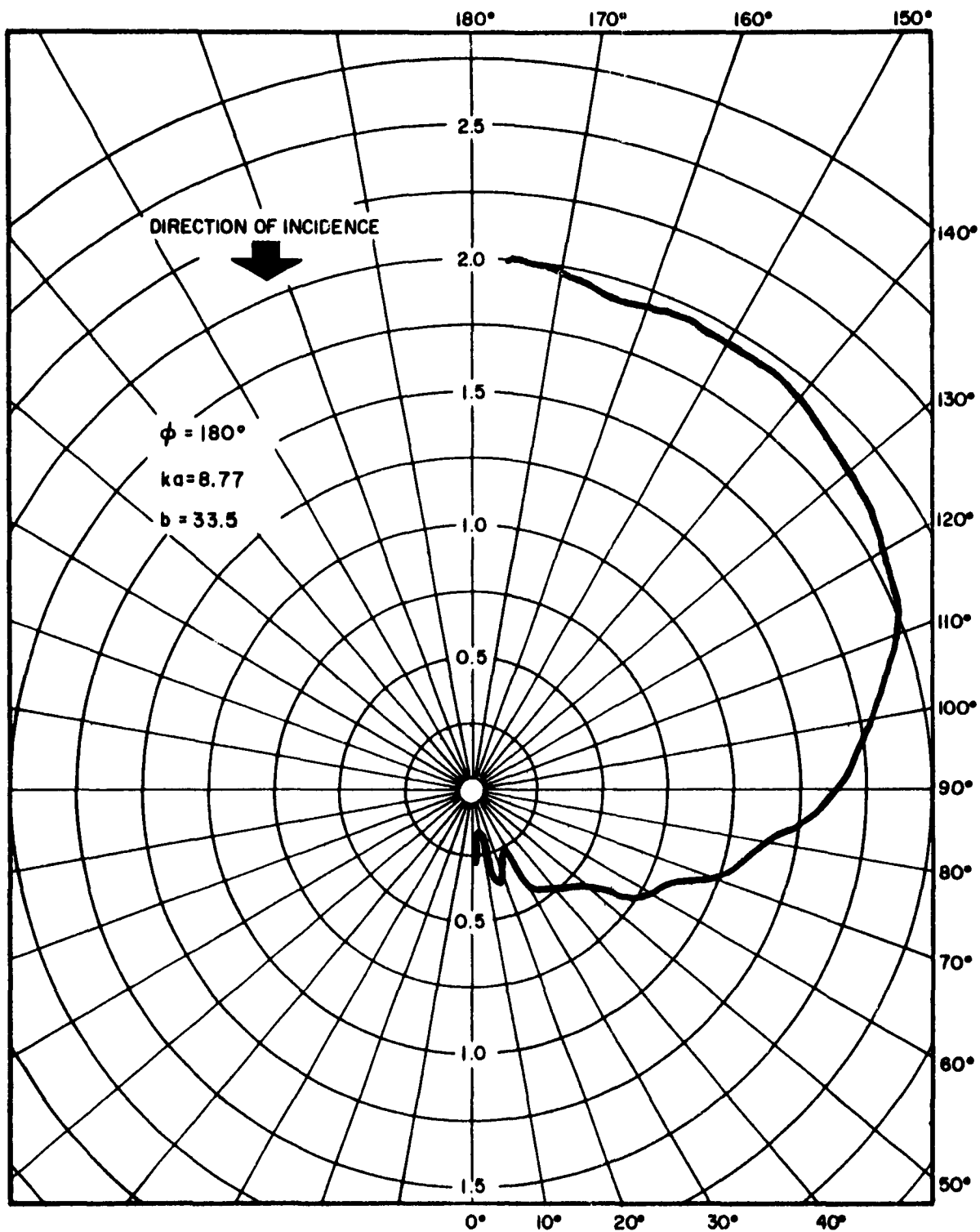


Fig. 4 - PRESSURE AMPLITUDE OF BAFFLE-TRANSDUCER SOUND FIELD AT THE TRANSDUCER FACE

REFERRED TO UNIT AMPLITUDE INCIDENT WAVE

TRACOR, INC. DWG. A2000-174
 AUSTIN, TEXAS 8/10/83 WCM/CWC

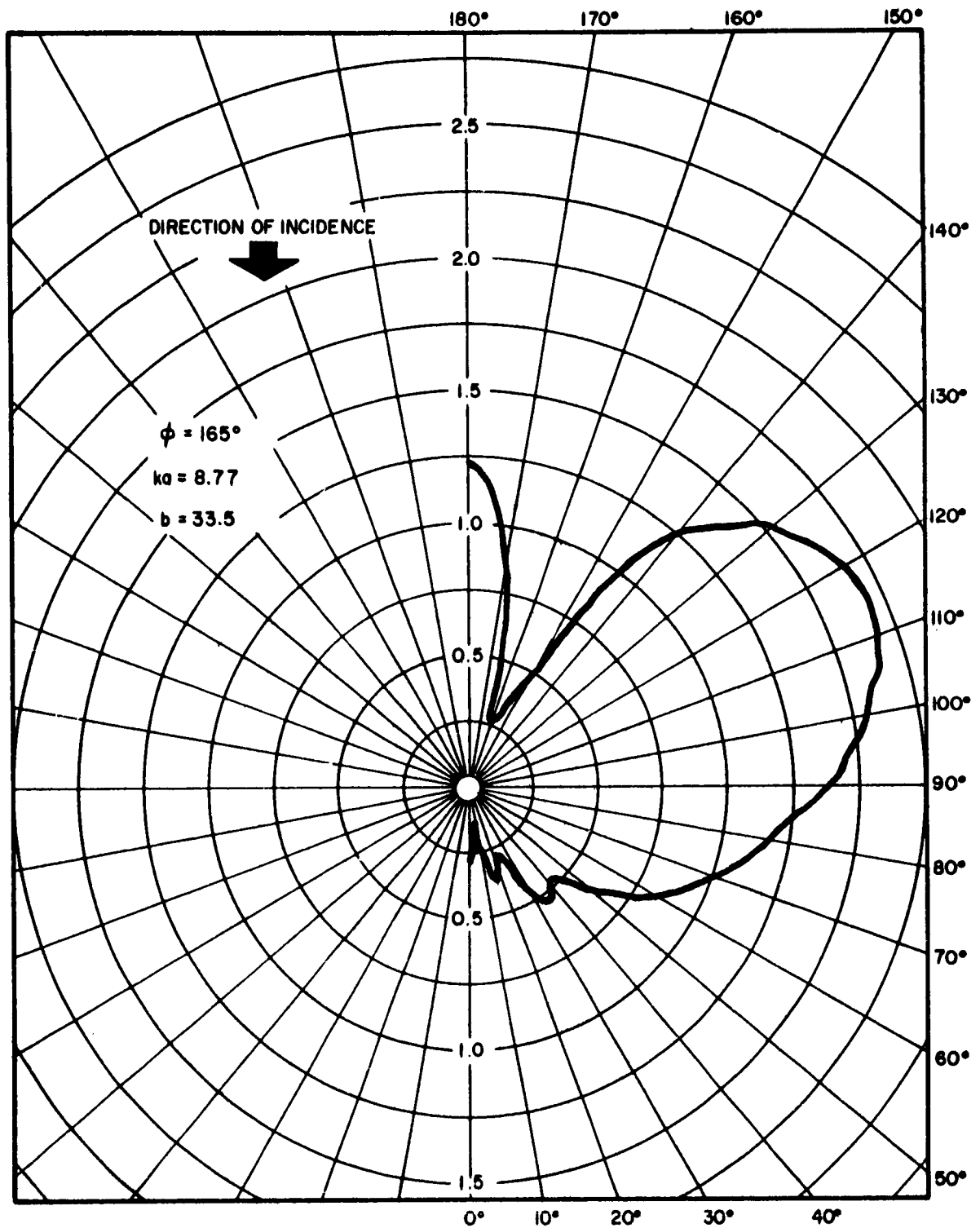


Fig. 5 - PRESSURE AMPLITUDE OF BAFFLE-TRANSDUCER SOUND FIELD AT THE TRANSDUCER FACE

REFERRED TO UNIT AMPLITUDE INCIDENT WAVE

TRACOR, INC. DWG. A2000-173
 AUSTIN, TEXAS 8/12/83 WCM/CWC

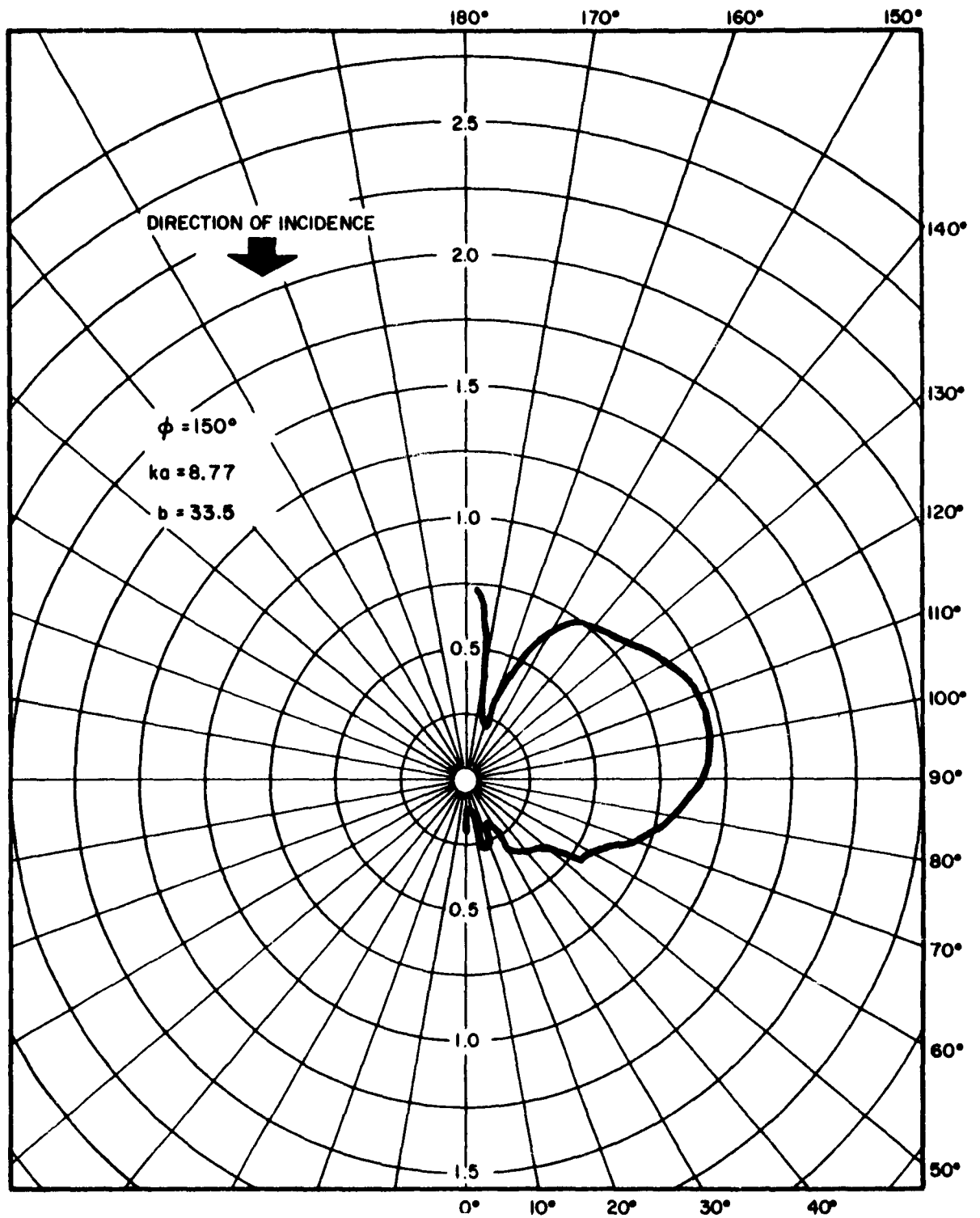


Fig. 6 - PRESSURE AMPLITUDE OF BAFFLE-TRANSDUCER SOUND FIELD AT THE TRANSDUCER FACE

REFERRED TO UNIT AMPLITUDE INCIDENT WAVE

TRACOR, INC. DWG. A2000-172
 AUSTIN, TEXAS 8/18/68 WGM/CWG

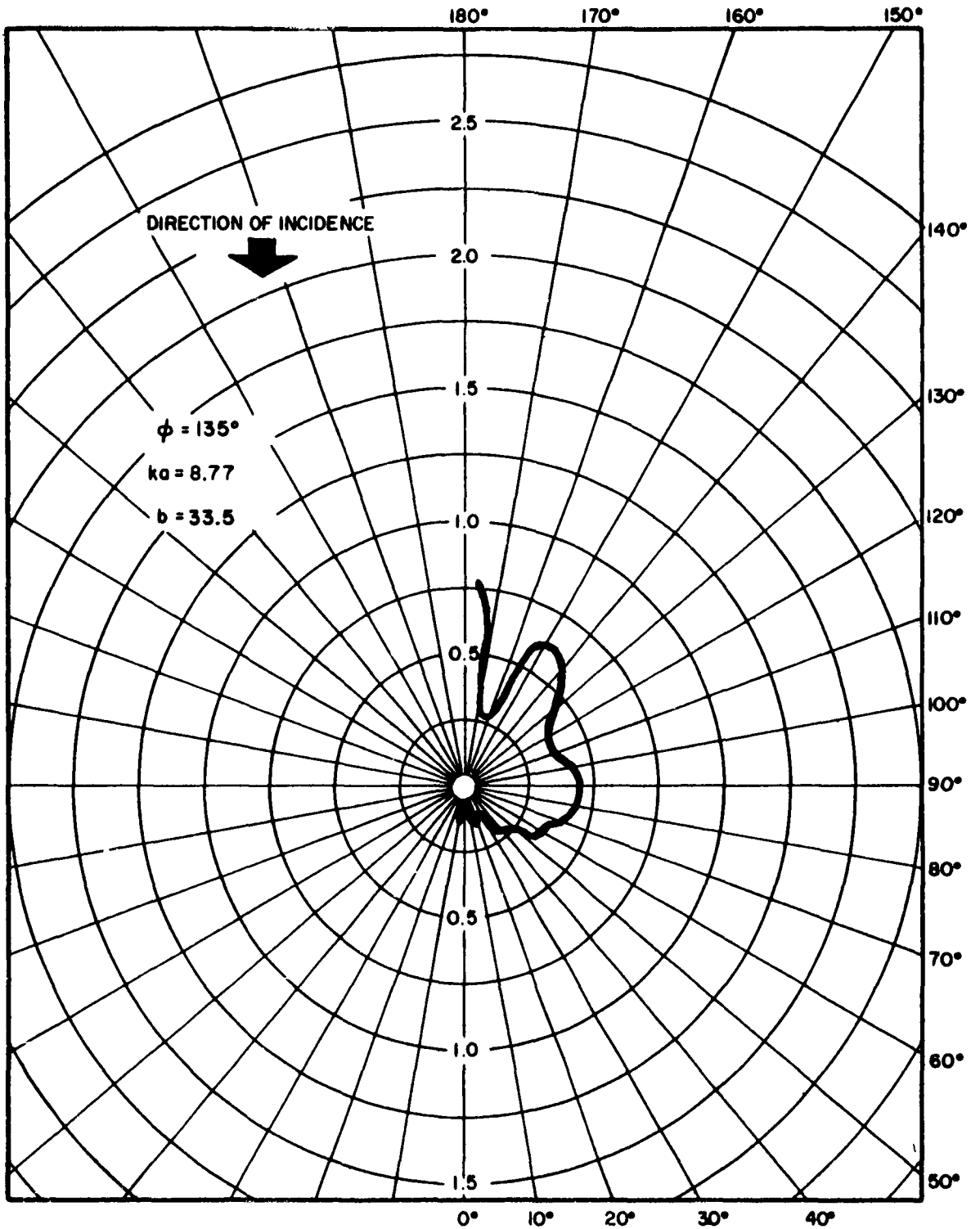


Fig. 7 - PRESSURE AMPLITUDE OF BAFFLE-TRANSDUCER SOUND FIELD AT THE TRANSDUCER FACE

REFERRED TO UNIT AMPLITUDE INCIDENT WAVE

TRACOR, INC. DWG. A2000-171
 AUSTIN, TEXAS 8/18/63 WCM /CWC

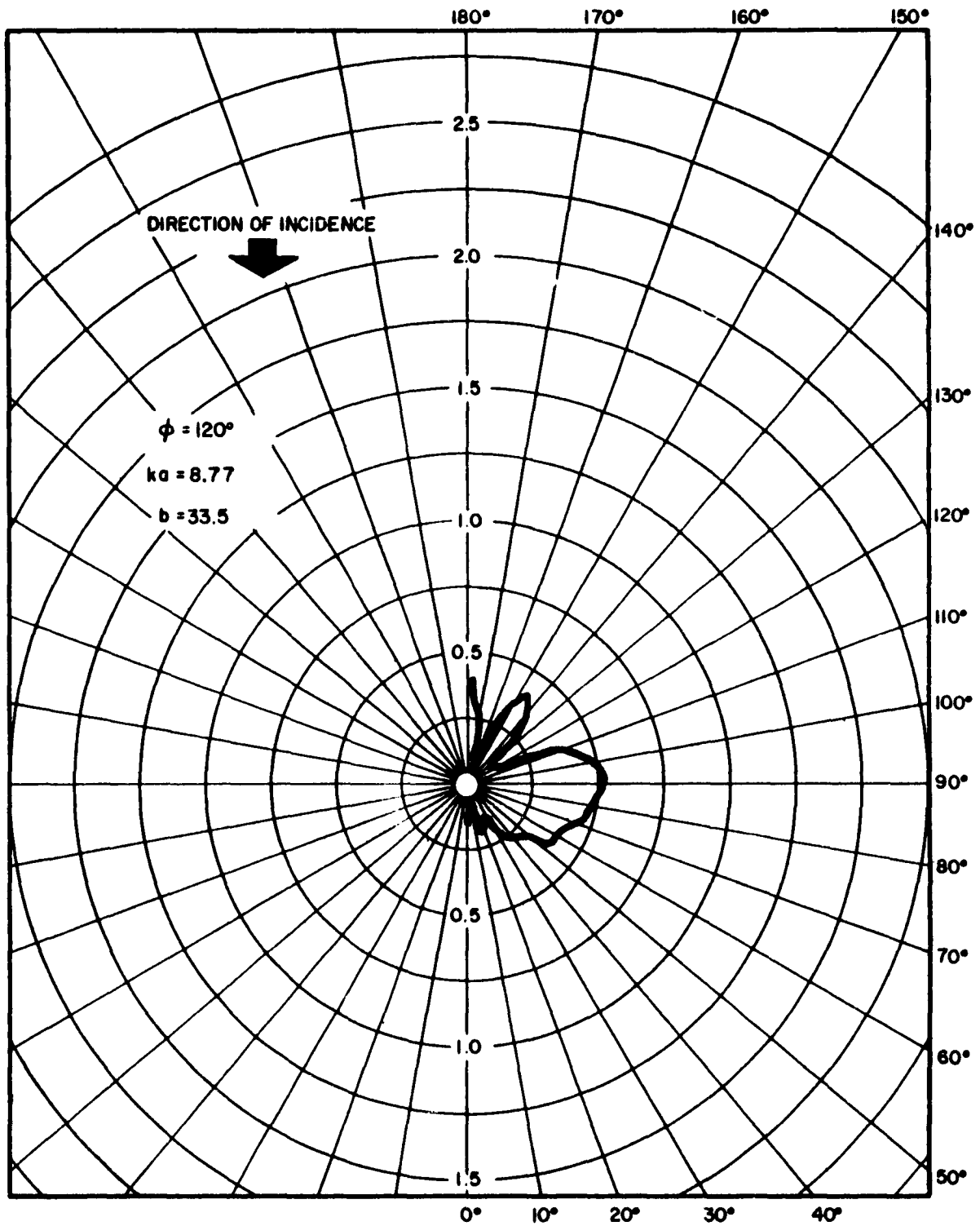


Fig. 8 - PRESSURE AMPLITUDE OF BAFFLE-TRANSDUCER SOUND FIELD AT THE TRANSDUCER FACE

REFERRED TO UNIT AMPLITUDE INCIDENT WAVE

TRACOR, INC. DWG. A2000-177
 AUSTIN, TEXAS 8/18/63 WGM/CWC

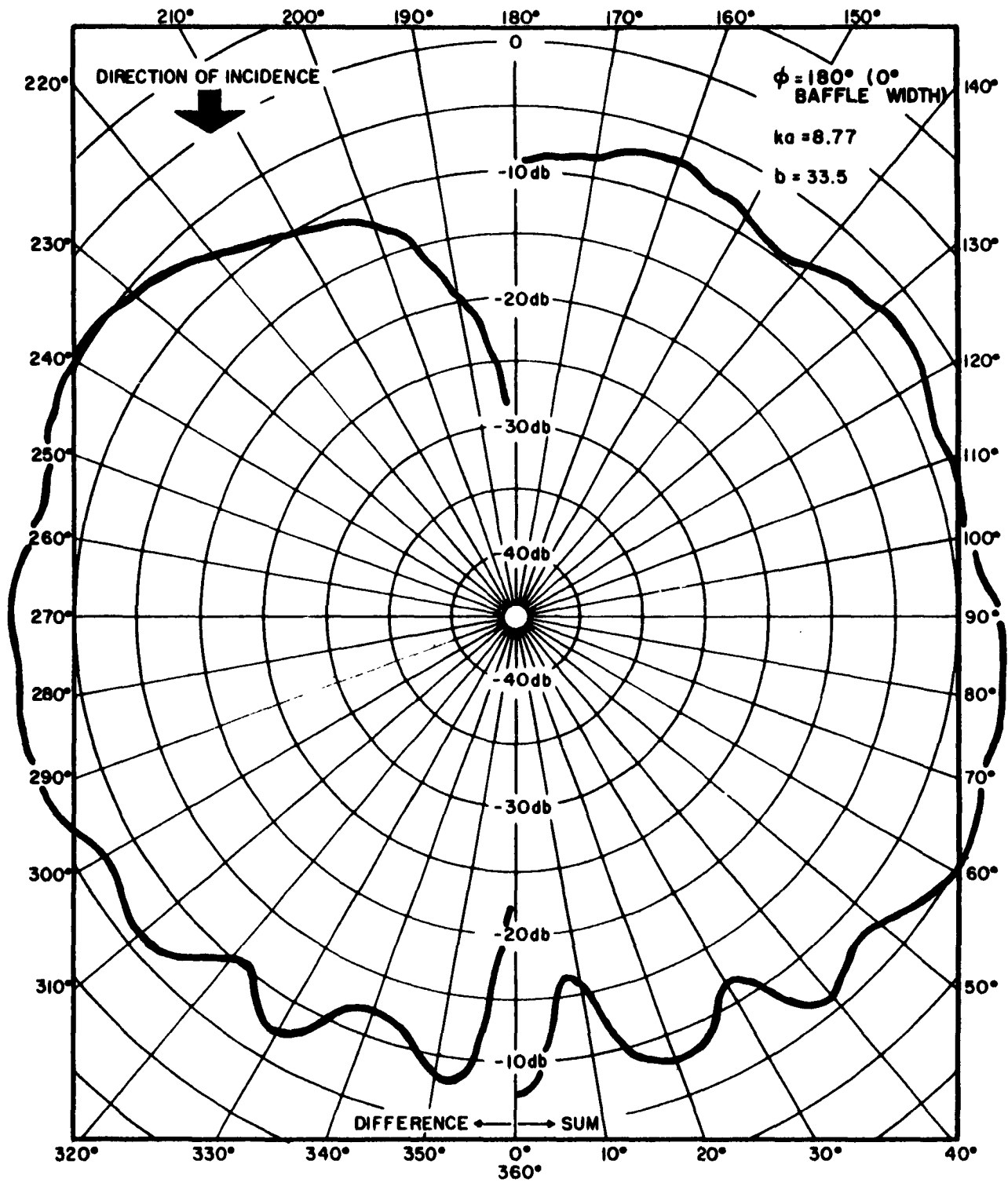


Fig. 9 -SELF-NOISE DIRECTIVITY PATTERN

REFERRED TO UNIT AMPLITUDE INCIDENT WAVE-db

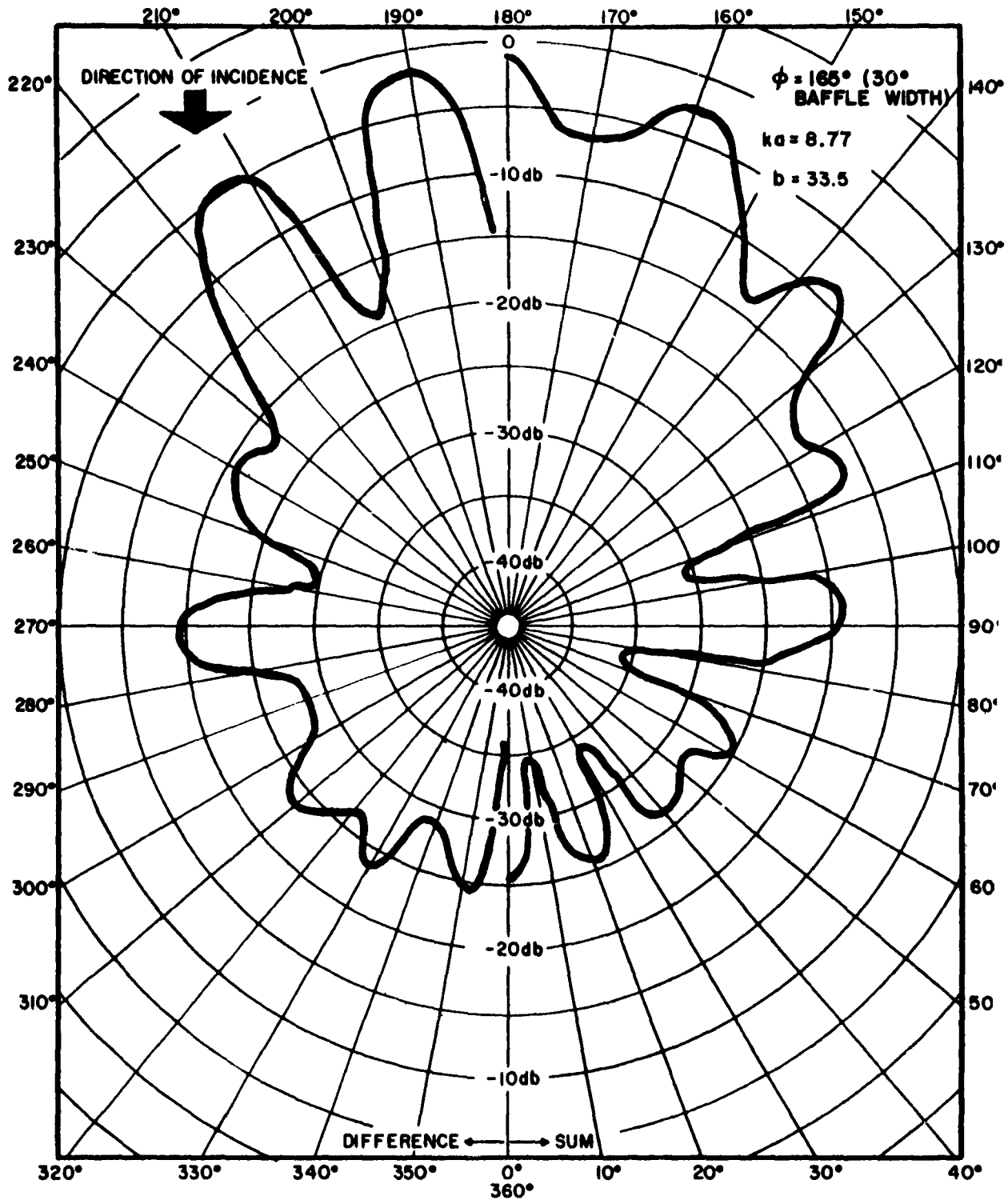


Fig.10 -SELF-NOISE DIRECTIVITY PATTERN

REFERRED TO UNIT AMPLITUDE INCIDENT WAVE-db

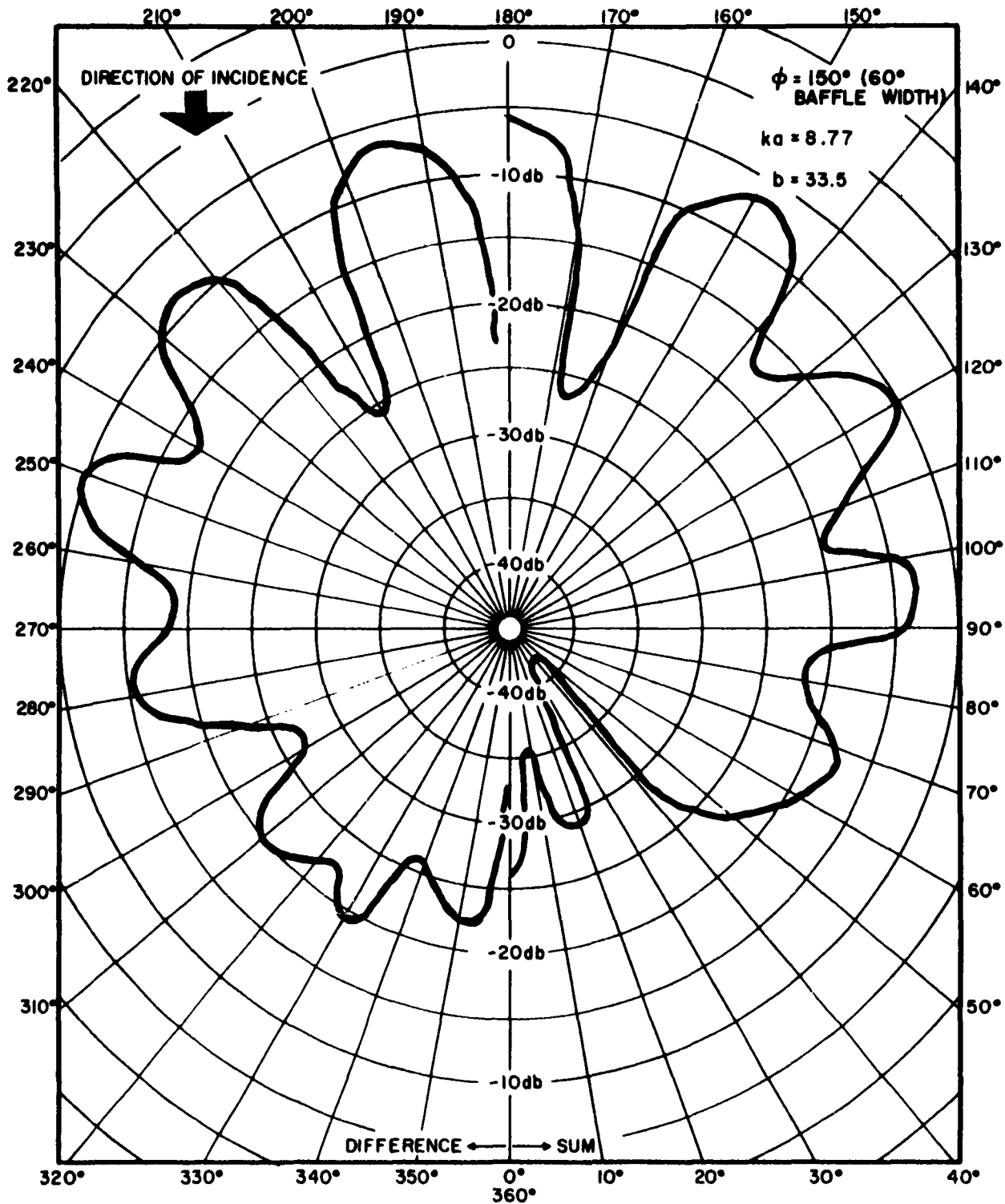


Fig. II -SELF-NOISE DIRECTIVITY PATTERN

REFERRED TO UNIT AMPLITUDE INCIDENT WAVE-db

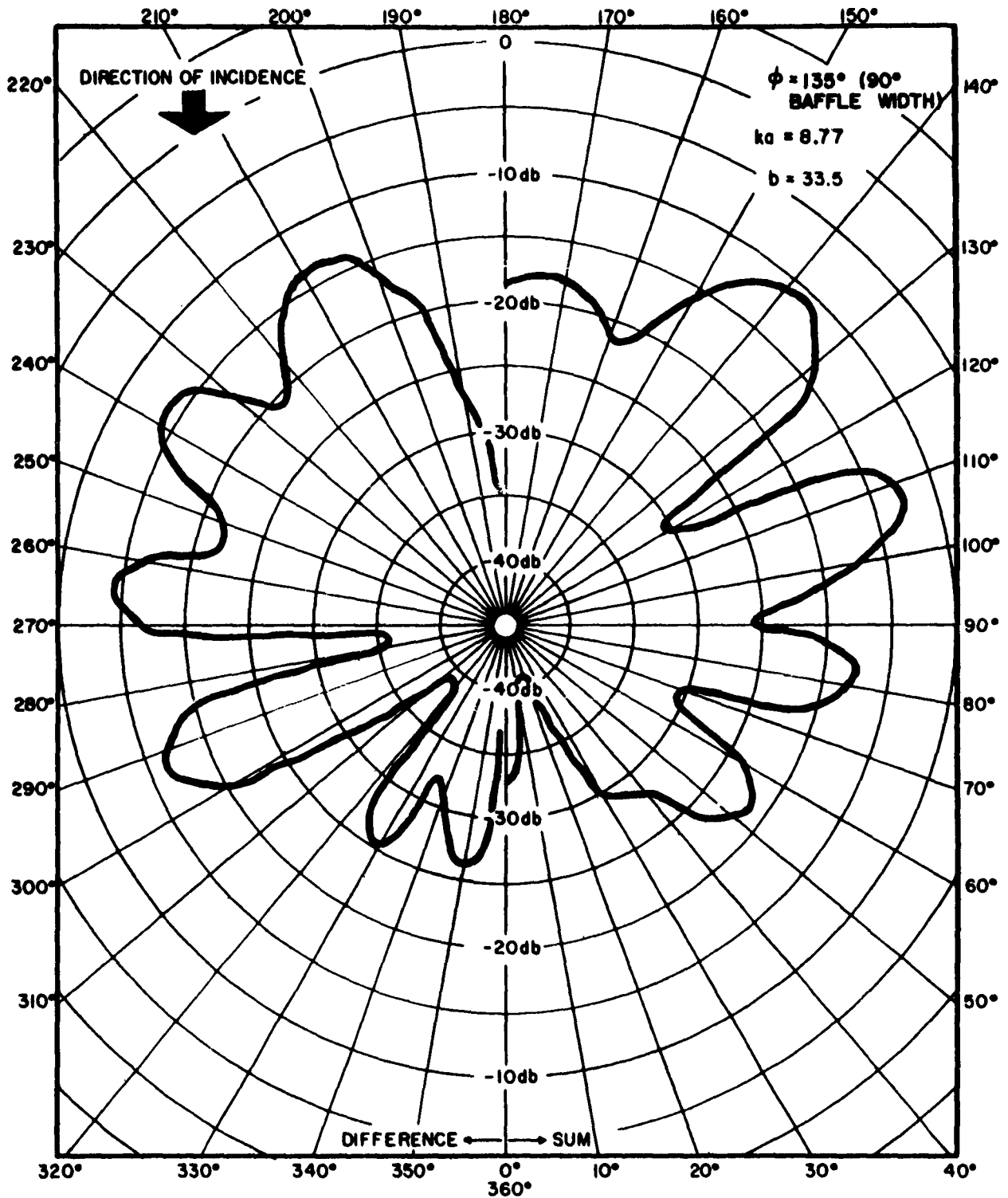


Fig.12 -SELF-NOISE DIRECTIVITY PATTERN

REFERRED TO UNIT AMPLITUDE INCIDENT WAVE-db

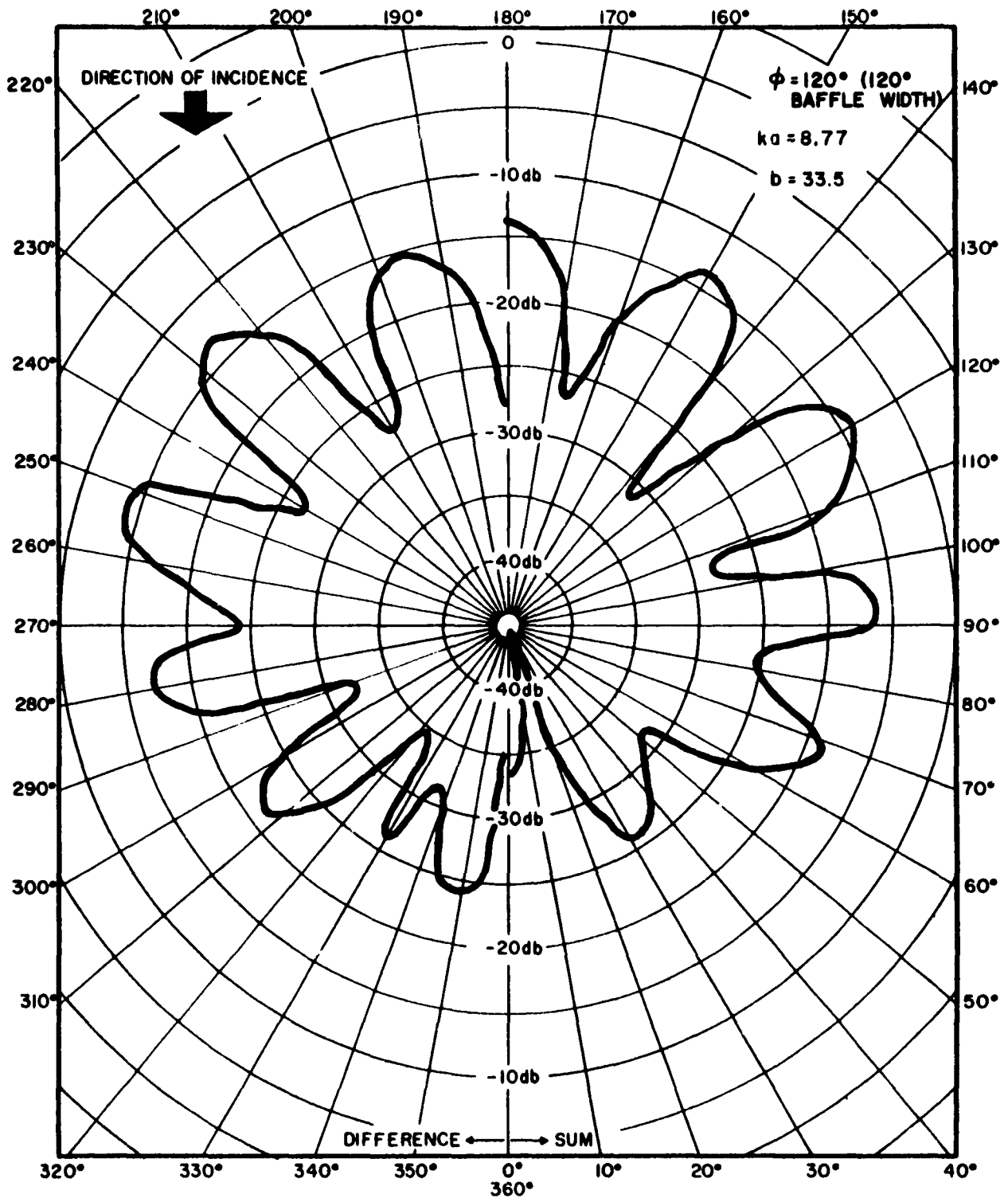


Fig. 13 -SELF-NOISE DIRECTIVITY PATTERN

REFERRED TO UNIT AMPLITUDE INCIDENT WAVE-db

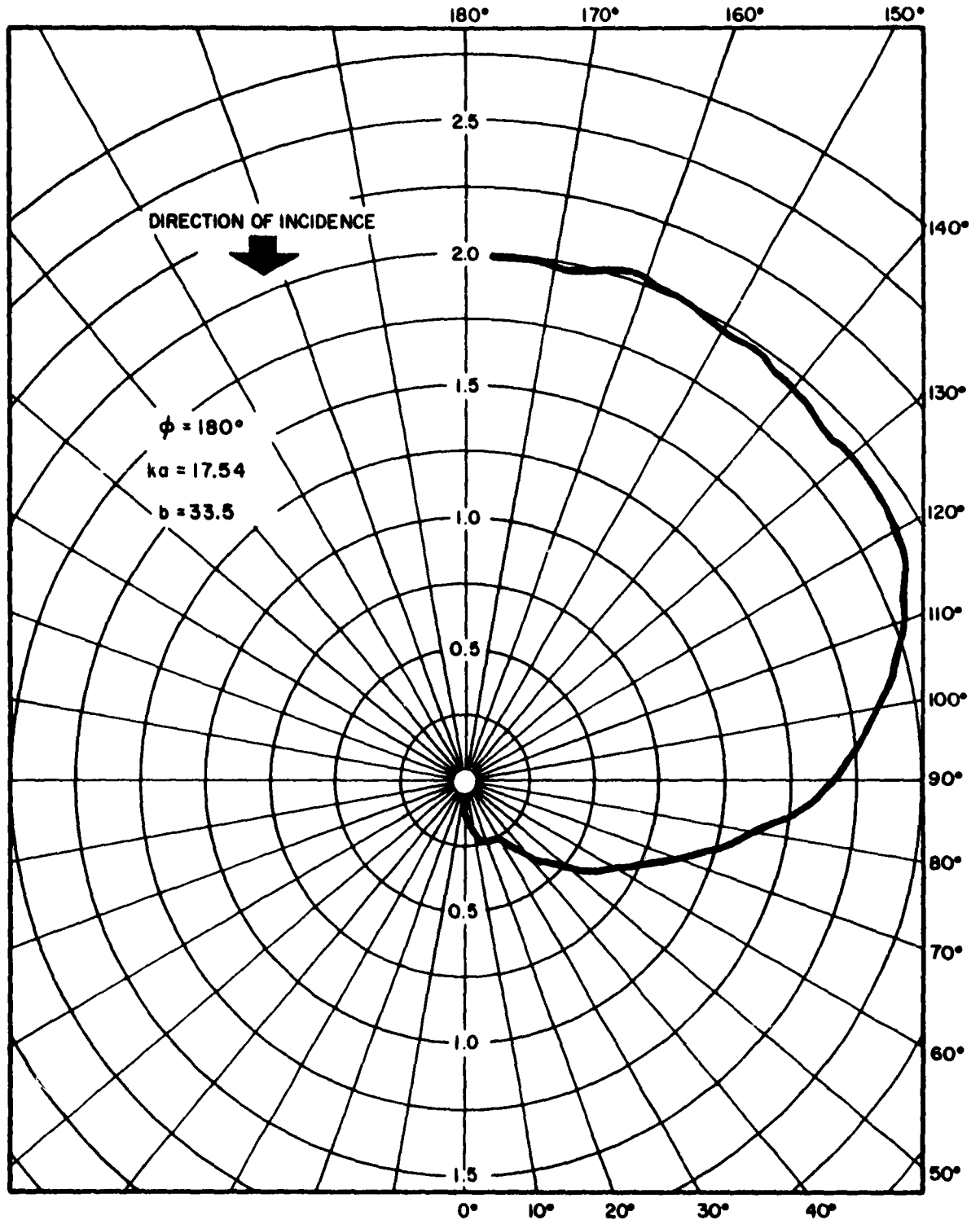


Fig.14 - PRESSURE AMPLITUDE OF BAFFLE-TRANSDUCER SOUND FIELD AT THE TRANSDUCER FACE

REFERRED TO UNIT AMPLITUDE INCIDENT WAVE

TRACOR, INC. DWG. A2000-170
 AUSTIN, TEXAS 8/18/83 WCM/CWC

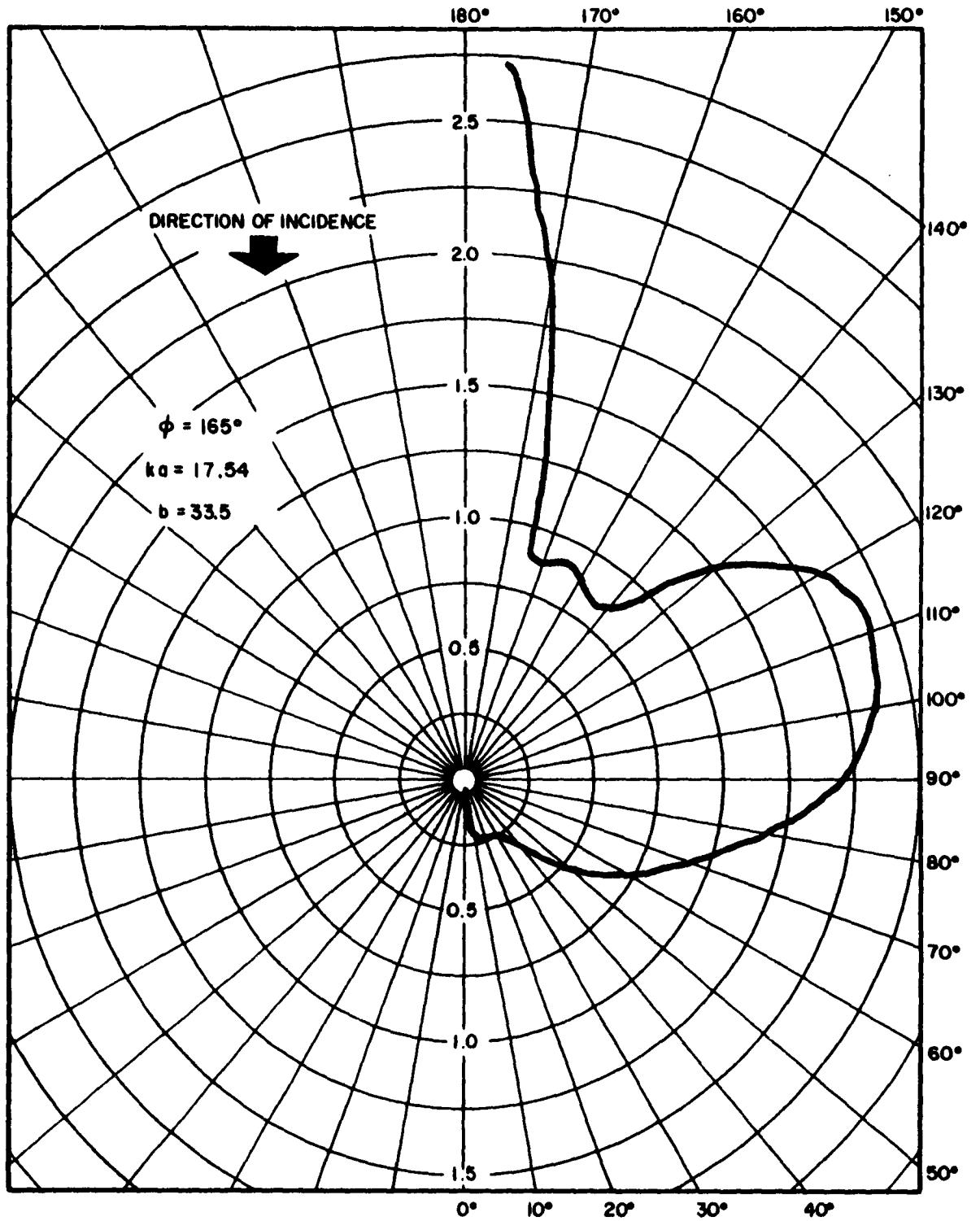


Fig.15 - PRESSURE AMPLITUDE OF BAFFLE-TRANSDUCER SOUND FIELD AT THE TRANSDUCER FACE

REFERRED TO UNIT AMPLITUDE INCIDENT WAVE

TRACOR, INC. DWG. A 2000-169
 AUSTIN, TEXAS 8/18/63 WCM/CWC

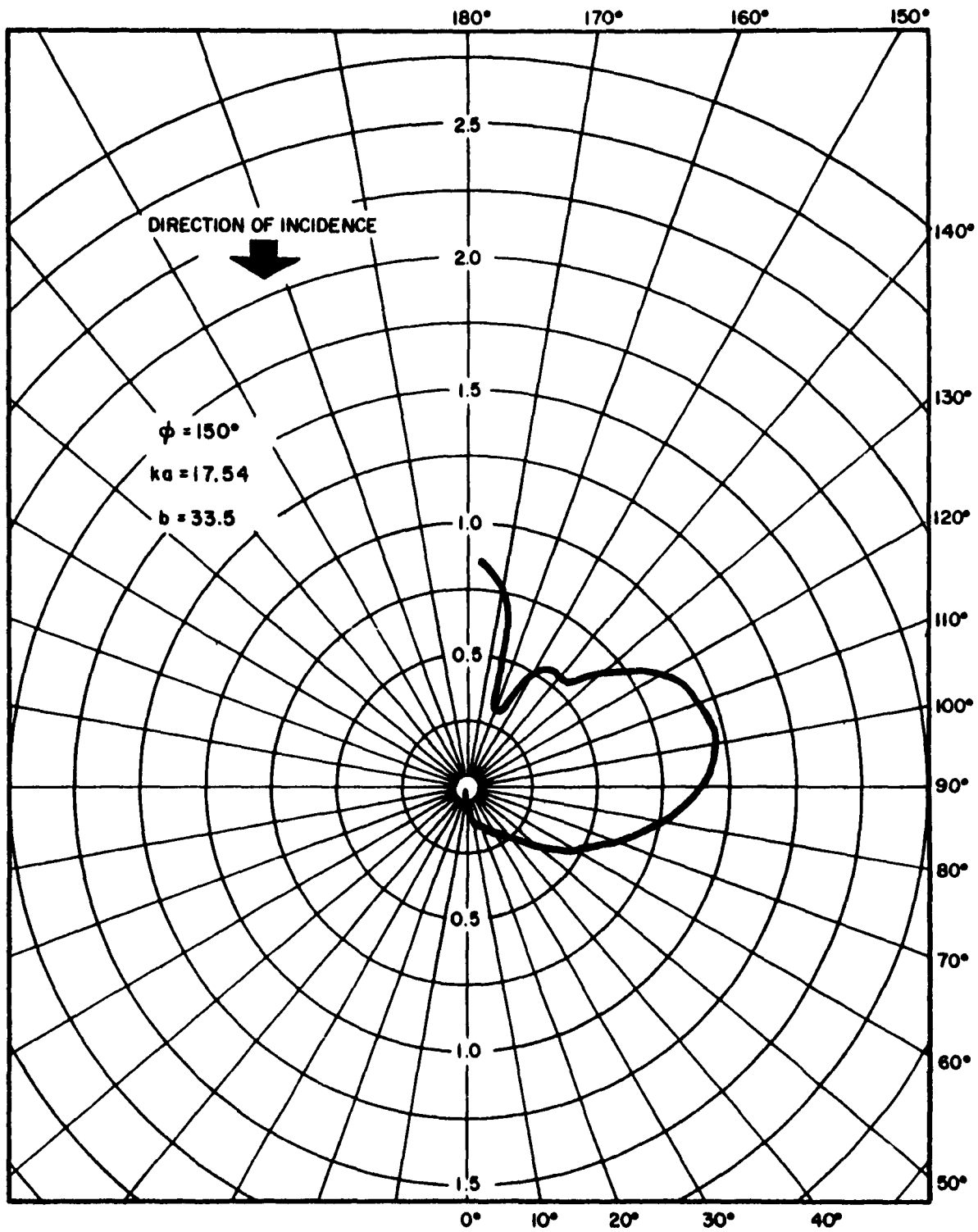


Fig.16 - PRESSURE AMPLITUDE OF BAFFLE-TRANSDUCER SOUND FIELD AT THE TRANSDUCER FACE

REFERRED TO UNIT AMPLITUDE INCIDENT WAVE

TRACOR, INC. DWG. A2000-188
 AUSTIN, TEXAS 6/16/69 WGM/6WG

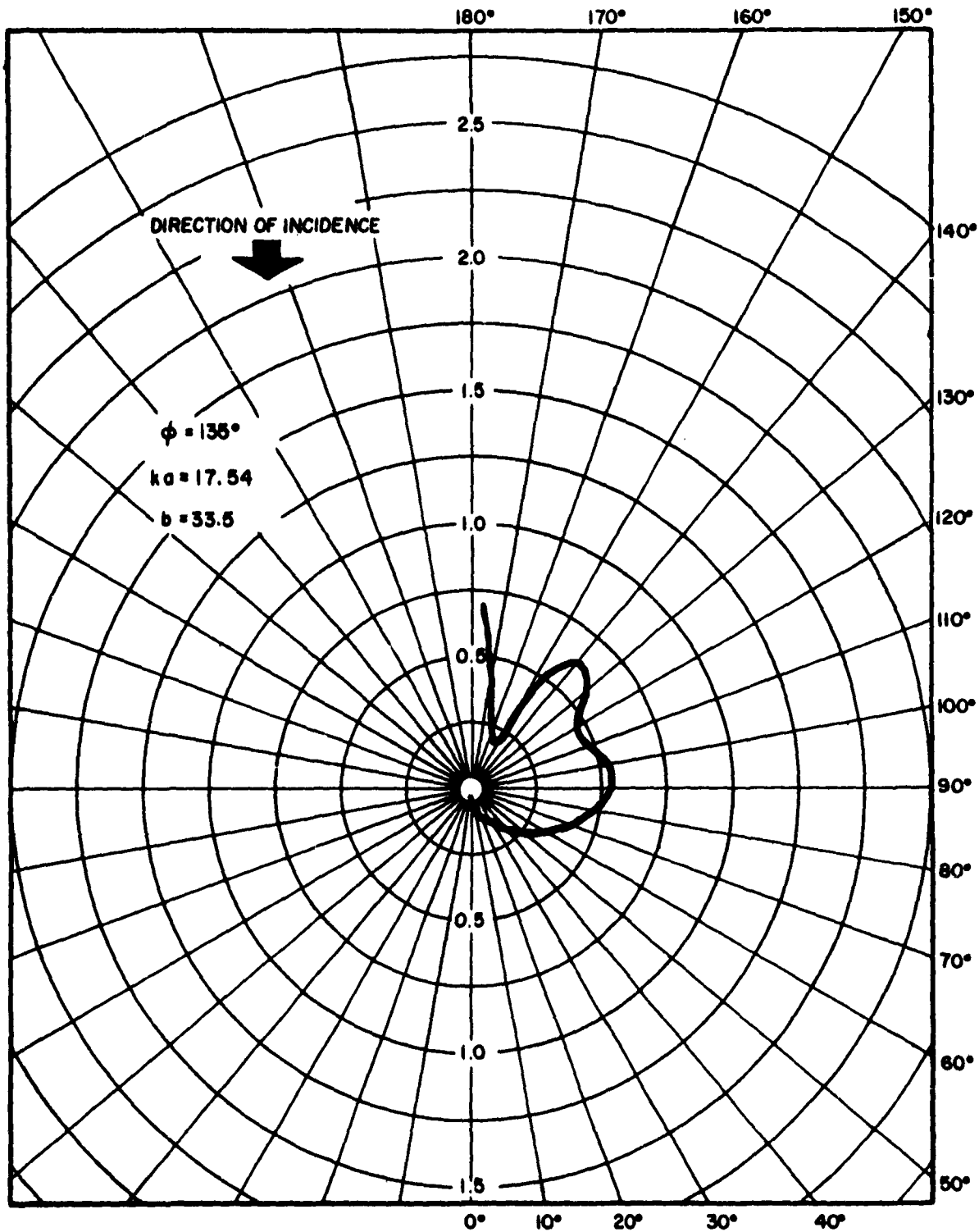


Fig.17 - PRESSURE AMPLITUDE OF BAFFLE-TRANSDUCER SOUND FIELD AT THE TRANSDUCER FACE

REFERRED TO UNIT AMPLITUDE INCIDENT WAVE

TRACOR, INC. DWG. A2000-167
 AUSTIN, TEXAS 6/16/63 WGM/CWG

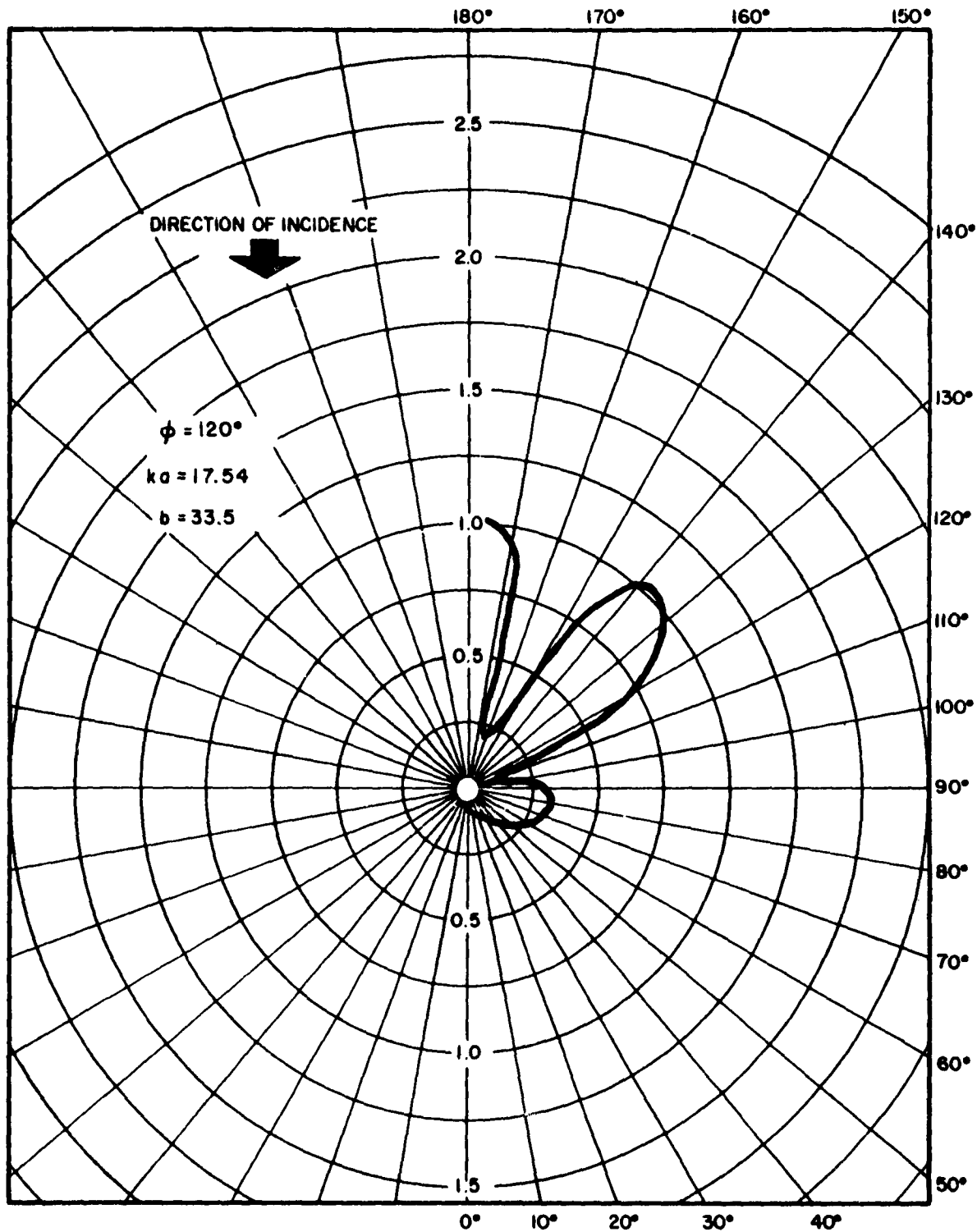


Fig.18 - PRESSURE AMPLITUDE OF BAFFLE-TRANSDUCER SOUND FIELD AT THE TRANSDUCER FACE

REFERRED TO UNIT AMPLITUDE INCIDENT WAVE

TRACOR, INC DWG. A2000-166
 AUSTIN, TEXAS 8/18/63 WCM/GWC

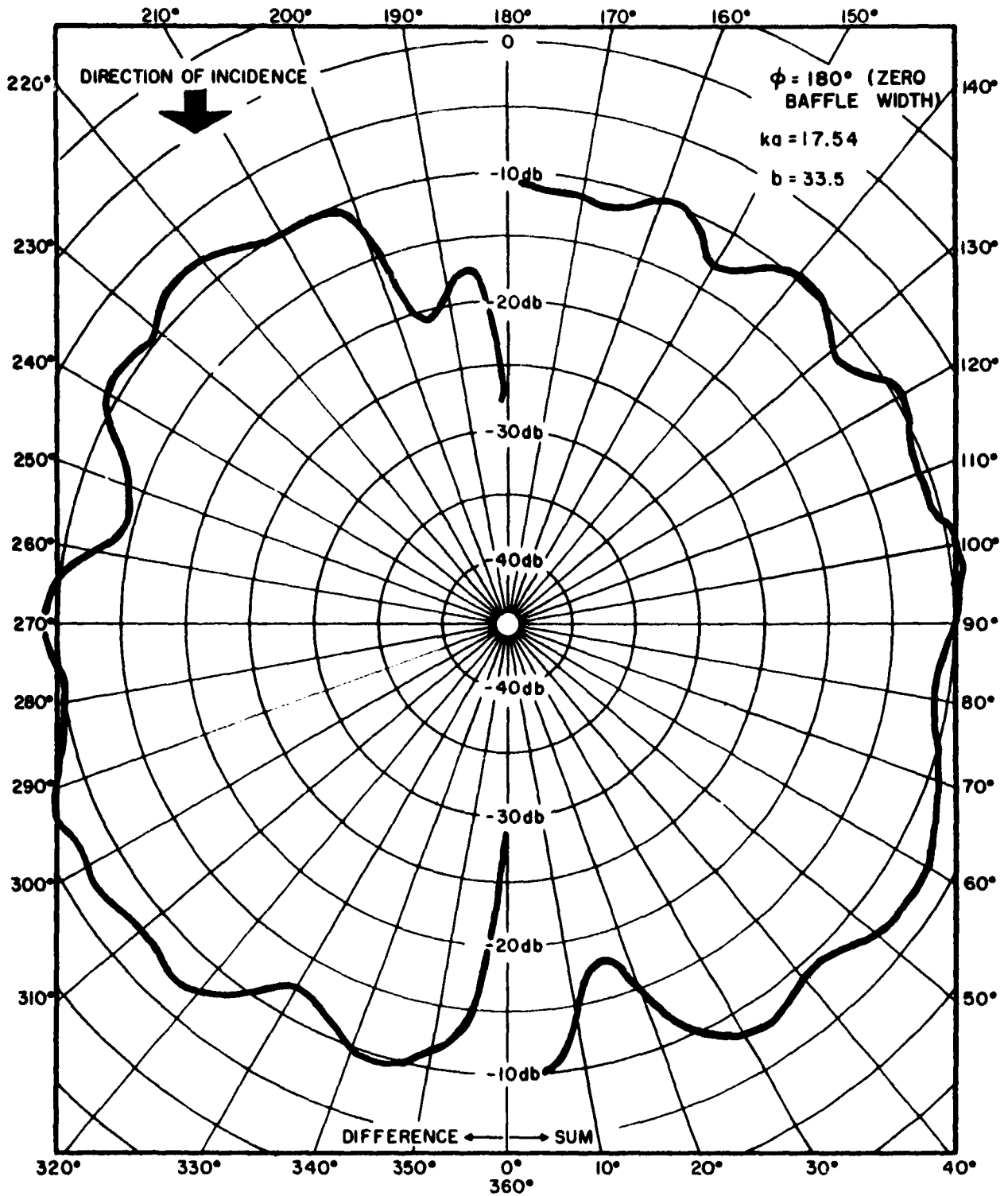


Fig.19 -SELF-NOISE DIRECTIVITY PATTERN

REFERRED TO UNIT AMPLITUDE INCIDENT WAVE-db

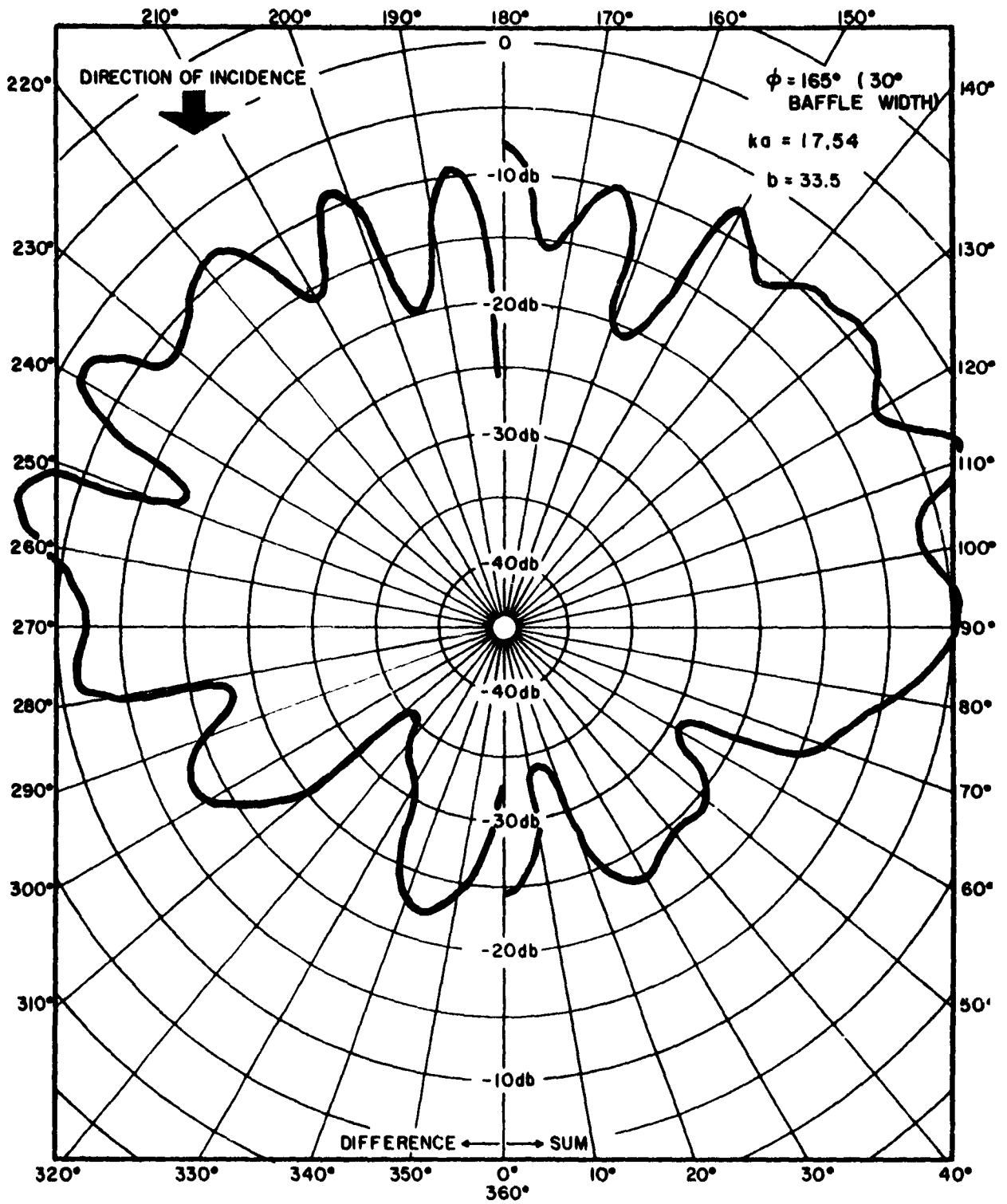


Fig.20-Self-Noise Directivity Pattern

REFERRED TO UNIT AMPLITUDE INCIDENT WAVE-db

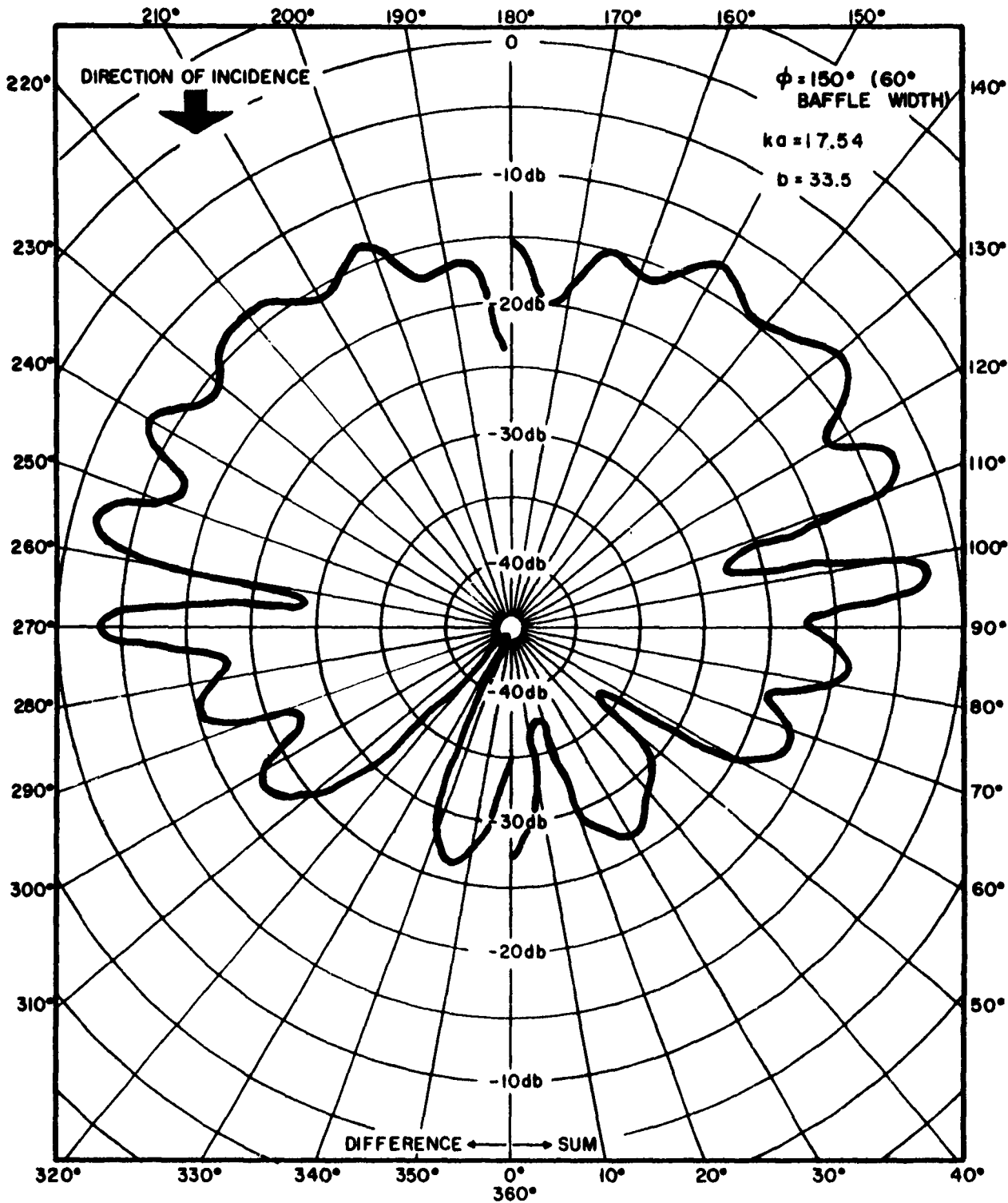


Fig.21 -SELF-NOISE DIRECTIVITY PATTERN

REFERRED TO UNIT AMPLITUDE INCIDENT WAVE-db

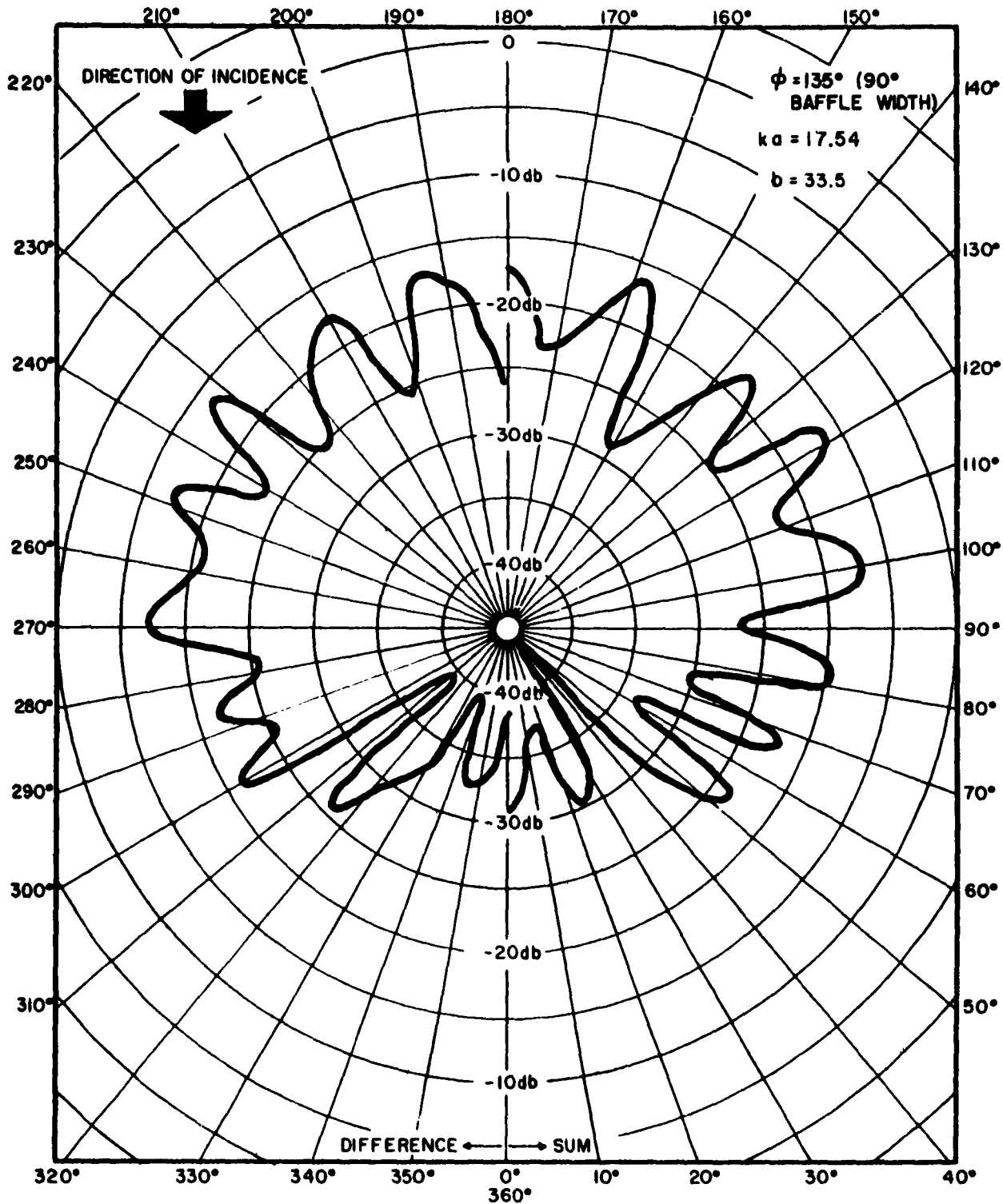


Fig.22 -SELF-NOISE DIRECTIVITY PATTERN

REFERRED TO UNIT AMPLITUDE INCIDENT WAVE-db

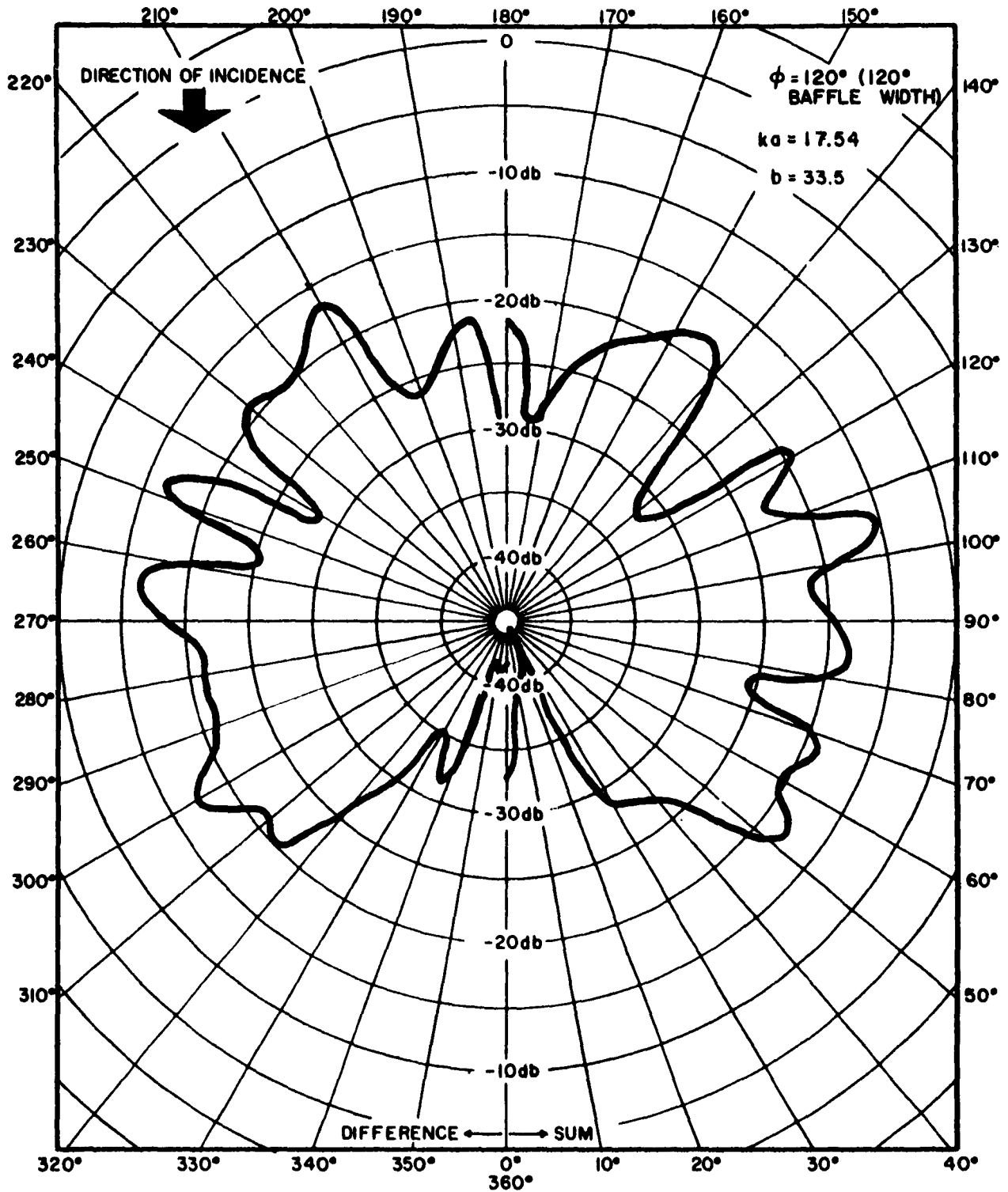


Fig.23-Self-Noise Directivity Pattern

REFERRED TO UNIT AMPLITUDE INCIDENT WAVE-db

APPENDIX A

SOLUTION OF A SET OF SIMULTANEOUS EQUATIONS

In order to evaluate the solution to the baffle-transducer sound field eq. (1), a set of simultaneous inhomogeneous equations must be solved. An argument has been presented for evaluating a finite-set of equations as an approximation to the infinite set presented in eq. (3). Here it is assumed that a finite set of simultaneous inhomogeneous equations is to be solved.

The finite approximation to the set of equations given in equations (10) and (11) can be represented in the form

$$a_{11}x_1 + a_{12}x_2 \cdots a_{1N}x_N = c_1$$

$$a_{21}x_1 + a_{22}x_2 \cdots a_{2N}x_N = c_2$$

·
·
·
·

$$a_{N1}x_1 + a_{N2}x_2 \cdots a_{NN}x_N = c_N$$

or

$$\sum_{j=1}^N a_{ij}x_j = c_i \quad i = 1, 2, 3 \cdots N$$

Consider any particular unknown x_j . Because of the limited number of significant digits available in the computer, it is desirable to choose the equation which depends most strongly on x_j to eliminate x_j from the remaining equations. In a physical sense this corresponds to measuring the quantity in a system which exhibits the greatest change with variations of a particular parameter of

the system in order to obtain the most accurate evaluation of the dependence of the system on the parameter. Therefore, the equation in which the magnitude of the coefficient of x_j is largest as compared to the sum of the magnitudes of the rest of the coefficients in that equation is chosen. (In actual practice the squares of the coefficients are used.) This process assures that the errors incurred in the additions and subtractions necessary to the evaluation of the x_j 's will be minimized.

In order to solve for x_j (initial J is 1), the following quantities are calculated for all i 's:

$$\beta_i = \sum_{j=J}^N (a_{ij})^2$$

A value of i , say I , is then chosen such that the quantity

$$\frac{(a_{iJ})^2}{\beta_i}$$

is maximized. After I has been determined, the quantities

$$a'_{Ij} = \frac{a_{Ij}}{a_{IJ}} \quad \text{and} \quad c'_I = \frac{c_I}{a_{IJ}}$$

are calculated for all j . Then, for $i \neq I$ and $j \geq J$, the quantities

$$a'_{ij} = a_{ij} - \frac{a_{Ij}}{a_{IJ}} a_{iJ}$$

$$c'_i = c_i - \frac{c_I}{a_{IJ}} a_{iJ}$$

are calculated, where $a'_{iJ} = 0$, and $a'_{ij} = a_{ij}$, $j < J$.

This operation reduces the coefficient of x_j in the I equation to 1 and reduces the coefficient of x_j in all of the other equations to zero. Now J is incremented by 1 and the process is repeated. After this process has been carried out for all J (1,2,3,...N) the matrix of coefficients has one and only one coefficient in each column equal to 1 and all other coefficients in that column are zero. The equations are then re-ordered along with the new inhomogeneities to get the matrix of coefficients in the form of the unit matrix, i.e., ones down the diagonal and zeros everywhere else so that,

$$\sum_{j=1}^N a'_{ij} x_j = c'_i$$

reduces to,

$$a'_{ii} x_i = c'_i = x_i ,$$

and the set of new inhomogeneities, c'_i , becomes the solution for the set of unknowns, x_i .

We were originally presented with a problem which may be written in matrix notation as

$$AX = C ,$$

where A is the matrix of coefficients, X is a column vector of the unknowns and C is a column vector of the inhomogeneities. We have now solved for X and obtained a solution, X' , which is not exact. Using X' and the original set of coefficients, A, a new set of inhomogeneities D can be determined.

$$AX' = D .$$

This equation is now multiplied by a constant k, which is to be determined, and subtracted from the original equation to get:

$$A(X - kX') = C - kD$$

We now wish to pick k so that the magnitude of the vector, C - kD, i.e., |C - kD| is minimized. We know that,

$$|C - kD|^2 = \sum_{i=1}^N (c_i - kd_i)^2 = \gamma ,$$

and to get γ a minimum with respect to k, γ must satisfy

$$\frac{d\gamma}{dk} = 0$$

or

$$\sum_{i=1}^N 2(c_i - kd_i) (-d_i) = 0$$

$$\sum_{i=1}^N c_i d_i - k \sum_{i=1}^N (d_i)^2 = 0$$

and it is seen that,

$$k = \frac{\sum_{i=1}^N c_i d_i}{\sum_{i=1}^N (d_i)^2}$$

Having determined k , the following is calculated.

$$x_i'' = kx_i'$$

$$c_i'' = kd ;$$

but

$$x_i' = c_i'$$

so that

$$x_i'' = kc_i'$$

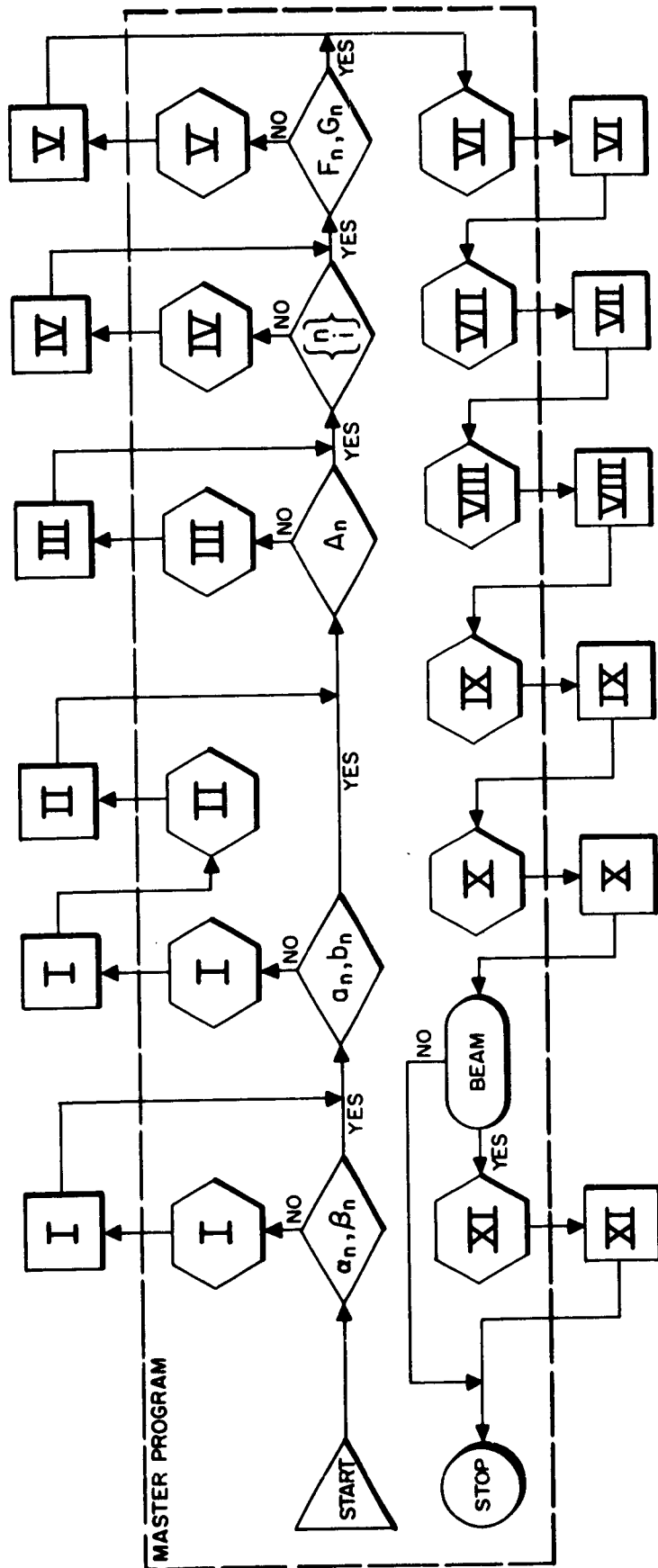
The x_i'' are taken to be the final solution to the set of simultaneous equations. These values are stored on magnetic tape and printed out along with the c_i'' and c_i' . The c_i'' and c_i' are printed out in order to determine how good a solution the x_i'' are.

APPENDIX B

PROGRAM DESCRIPTION

The numerical evaluation of the baffle-transducer sound field, eq. (1) is accomplished using a master control program that reads the required sub-routines into the computer and stores the results of these computations for use in subsequent sub-routines. The evaluation of each of the quantities described in Section II is accomplished with a sub-routine of the master control program. A flow chart for the computer program is given in Figure 1B. A description of the various sub-routines is given below. Roman numerals identify the various sub-routines that appear on the flow chart.

- I. Reads k and x ($x=a$ or b) from paper tape and calculates $J_n(kx)$, $N_n(kx)$, $J'_n(kx)$, and $N'_n(kx)$. Stores all four sets of values in separate files on magnetic tape.
- II. Reads a_n , b_n , $J_n(kb)$, and $N_n(kb)$ from magnetic tape and calculates L_n and M_n . Stores both sets of values in separate files on magnetic tape.
- III. Reads a_n , b_n , α_n , and β_n from magnetic tape and calculates A_n . Stores set of values in one file on magnetic tape.
- IV. Reads φ from paper tape and calculates $\left\{ \begin{matrix} n \\ j \end{matrix} \right\}$. Stores all values in one file on magnetic tape.
- V. Reads L_n , b_n , a_n , and $\left\{ \begin{matrix} n \\ j \end{matrix} \right\}$ from magnetic tape, φ from paper tape and calculates F_n and G_n . Stores both sets of values in separate files on magnetic tape.
- VI. Reads $J_n(kb)$, $N_n(kb)$, α_n , and β_n from magnetic tape, φ from paper tape and calculates B_n . Stores all values in one file on magnetic tape.



XY DENOTES: ARE THE DESIRED VALUES OF X AND Y ON MAGNETIC TAPE

Y DENOTES: READ SUBROUTINE Y FROM MAGNETIC TAPE

Y DENOTES: EXECUTE SUBROUTINE Y AS DESCRIBED

BEAM DENOTES: ARE BEAM; PATTERNS DESIRED



Fig. 1 B - COMPUTER DIAGRAM FLOW CHART

- VII. Reads M_n , L_n , α_n , β_n , and $\left\{ \begin{matrix} n \\ j \end{matrix} \right\}$ from magnetic tape and calculates X_ℓ^n and Y_ℓ^n . Stores blocks of X_ℓ^n and Y_ℓ^n alternately in one file on magnetic tape.
- VIII. Reads A_n , B_n , α_n , β_n , X_ℓ^n , Y_ℓ^n , F_n , and G_n from magnetic tape and forms matrix of coefficients of the D_n^R and D_n^I by columns. Stores each column as a block on magnetic tape all in one file. Last block in file consists of inhomogeneities (F_n & G_n).
- IX. Reads matrix of coefficients from magnetic tape and solves set of simultaneous equations for the D_n^R and D_n^I . Stores values of D_n^R and D_n^I alternately on magnetic tape in one file. Also prints out D_n^R , D_n^I , F_n , G_n and F'_n and G'_n calculated from the solution. (See Appendix A.)
- X. Reads D_n^R , D_n^I , α_n , and β_n from magnetic tape, k , r , and θ from paper tape, and calculates $|p_1|$ and ϕ for desired values of r and θ . Prints out $|p_1|$ and ϕ and if directivity patterns are desired, stores $|p_1|$ and ϕ on magnetic tape in one file.
- XI. Reads $|p_1|$ and ϕ from magnetic tape and calculates sum and difference self-noise directivity patterns. (See Appendix C.)

APPENDIX C

BEAM FORMING PROGRAM

The values for $|p_1|$ and φ which are obtained from eq. (1) are stored on magnetic tape so that they may be used as input data in a scanning sonar beam forming program. The values of $|p_1|$ and φ are obtained for points on the transducer which correspond to transducer elements. The beam forming program duplicates the actual sonar equipment process of vectorially summing responses of the elements to the right and to the left of the center of the beam. These sums are then added and subtracted to obtain sum and difference signals. The magnitude of the sum and difference signals are then considered the beam response to the incident sound field.

The analytical expression for the sum and difference signals is written as:

$$|P^L \pm P^R| = \left[\left(\sum_{n=1}^{N/2} |p_1|_n^L \cos \psi_n^L \pm \sum_{n=1}^{N/2} |p_1|_n^R \cos \psi_n^R \right)^2 + \left(\sum_{n=1}^{N/2} |p_1|_n^L \sin \psi_n^L \pm \sum_{n=1}^{N/2} |p_1|_n^R \sin \psi_n^L \right)^2 \right]^{\frac{1}{2}}$$

where N is the total number of elements used in forming the beam,

P^L = vectorial sum of pressures on the left of the beam center,

P^R = vectorial sum of pressures on the right of the beam center,

$|p_1|_n^L$ = value of $|p_1|$ at an angle θ_n on the left,

$|p_1|_n^R$ = value of $|p_1|$ at an angle θ_n on the right,

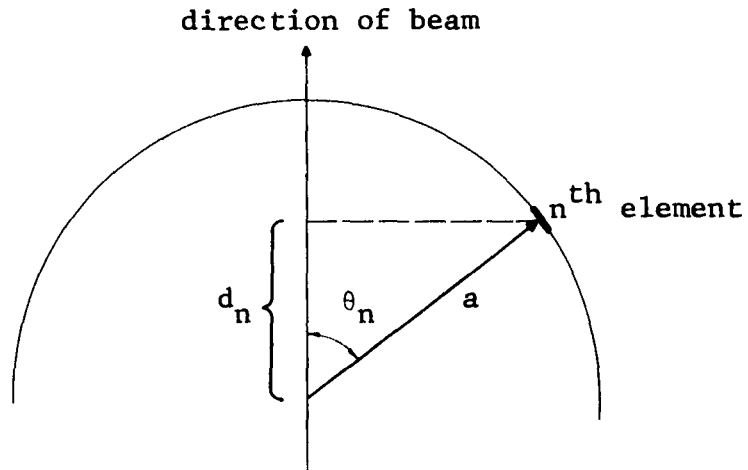
$$\psi_n^L = \varphi_n^L - \omega t_n$$

$$\psi_n^R = \varphi_n^R - \omega t_n$$

φ_n^L = value of φ at an angle θ_n on the left

φ_n^R = value of φ at an angle θ_n on the right

t_n is the delay time for an element at an angle θ_n on either side of the center of the beam which adjusts the phase at the n^{th} element (at the angle θ_n) so that all of the elements appear to be in a straight line perpendicular to the direction of the beam.



$$t_n = \frac{d_n}{c} = \frac{a \cos \theta_n}{c} \quad \text{and}$$

$$\omega t_n = 2\pi f \frac{a \cos \theta_n}{c} = \frac{2\pi a \cos \theta_n}{\lambda} = ka \cos \theta_n \quad ,$$

where c is the speed of sound.

θ_n corresponds to the direction of the beam lying between the elements. The number of elements used in forming the beam may be varied from a maximum of 24 down to 0.

In addition to printing out the values of $|P^L \pm P^R|$ corresponding to the beam being directed between every pair of elements on the transducer, these values are normalized by dividing by the number of elements, N, in the beam and these values are printed out in db:

$$|P^L \pm P^R| \text{ db.} = 20 \log_{10} \frac{|P^L \pm P^R|}{N}$$

In order to simplify the indexing of the various quantities involved in calculating $|P^L \pm P^R|$ the beam is taken to be directed in the direction $\theta = 90^\circ$ (See Figure 1) initially and successive values correspond to θ being incremented by 7.5° .

REFERENCES

1. TRACOR Technical Memorandum, "An Analytic Solution to the Sound Pressure Field Resulting From a Plane Wave Incident on a Cylinder and Concentric Cylindrical Section," March 14, 1963.
2. TRACOR Technical Memorandum, "The Evaluation of Bessel and Neumann Functions Through the Use of Taylor Series Solutions to Bessel's Differential Equation," December 3, 1962.
3. TRACOR Technical Memorandum, "Computation of Bessel and Neumann Functions," December 11, 1962.